Equilibrium Structures of Three-, Four-, Five-, Six-, and Seven-Membered Unsaturated N-Containing Heterocycles

ARTICLE *in* THE JOURNAL OF PHYSICAL CHEMISTRY A · OCTOBER 2014

Impact Factor: 2.69 · DOI: 10.1021/jp5084168 · Source: PubMed

3 AUTHORS, INCLUDING:

Attila Csaszar
Eötvös Loránd University
197 PUBLICATIONS **5,715** CITATIONS
SEE PROFILE

Heinz Dieter Rudolph
Universität Ulm
112 PUBLICATIONS **1,254** CITATIONS
SEE PROFILE

THE JOURNAL OF PHYSICAL CHEMISTRY A

Article

pubs.acs.org/JPCA

Equilibrium Structures of Three-, Four-, Five-, Six-, and Seven-Membered Unsaturated N-Containing Heterocycles

Attila G. Császár,*[,†,‡] Jean Demaison,[§] and Heinz Dieter Rudolph[∥]

[†]Laboratory of Molecular Structure and Dynamics, Eötvös University, H-1117 Budapest, Pázmány Péter sétány 1/A, Budapest, Hungary

[‡]MTA-ELTE Research Group on Complex Chemical Systems, H-1518 Budapest 112, P.O. Box 32, Budapest, Hungary

[§]Laboratoire de Physique des Lasers, Atomes et Molécules, Université de Lille I, 59655 Villeneuve d'Ascq Cedex, France

[∥]Department of Chemistry, University of Ulm, D-89069 Ulm, Germany

Supporting Information

ABSTRACT: Up to six different techniques are utilized to estimate the equilibrium structures (r_e) of a series of mostly unsaturated, N-containing heterocycles. Accurate Born−Oppenheimer (r_e^{BO}) and, if allowed, semiexperimental (r_e^{SE}), as well as empirical (r_m-type) estimates of the equilibrium structures of three-membered (1*H*- and 2*H*-azirine, aziridine), four-membered (azete), five-membered (pyrrole, pyrazole, imidazole), six-membered (pyridine, pyrimidine, uracil), and seven-membered (1*H*-azepine) rings, containing usually one but in some cases two N atoms, are determined. The agreement among the structural results of the different techniques is very satisfactory. It is shown that it is possible to use the CCSD(T) electronic structure method with the relatively small wCVTZ basis set, with all electrons correlated, and the effect of further basis set enlargement, wCVTZ → wCVQZ, computed at the MP2 level, to obtain reliable equilibrium structures for the semirigid molecules investigated. Extension to larger basis sets does not significantly improve the accuracy of the computed results. Although all molecules investigated are oblate, and their principal axis system is subject to large rotations upon isotopic substitution, the semiexperimental method, when applicable, provides accurate results, though in the difficult cases it must be augmented with the mixed regression method. Finally, it is noteworthy that the empirical mass-dependent (r_m) method also delivers surprisingly accurate structures for this class of compounds.

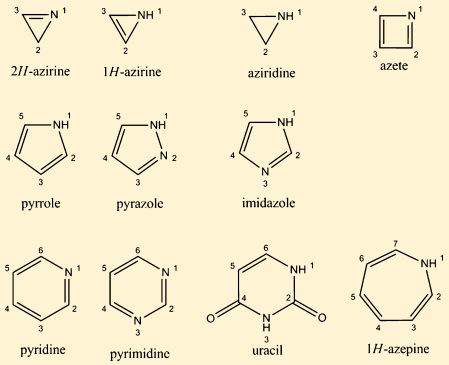

1. INTRODUCTION

The CN bond, along with the CC bond, has a central role in organic chemistry and biochemistry. The equilibrium length (r_e) of the C≡N triple bond in nitriles is well-established at about 1.15 Å,[1] and it does not vary much in different chemical environments. The variation of r_e(C≡N) is between 1.153 Å in HCN[2] and 1.160 Å in HCC−CN,[3] similarly constrained as the variation of the length of the C≡C triple bond. To wit, compare r_e(C≡N) in HCN with that in benzonitrile (1.158 Å)[4] and r_e(C≡C) in C_2H_2 (1.203 Å)[5] with that in phenylacetylene (1.207 Å).[4] In clear contrast, the length of the C═N double bond and especially that of the C−N single bond is extremely variable, ranging from 1.35 to 1.55 Å.[6] For example, the mean length of the C−N single bond is 1.46 Å,[7] but it varies from 1.348 Å in NH_2CN[6] to 1.55 Å in azete (see section 3 of this paper).

Structures of N-containing heterocycles of varying size and composition are interesting from several aspects. Heterocycles have determining roles in biochemistry, life sciences, and materials chemistry. Some of the interest also arises from structural underpinnings of chemical concepts like aromaticity, nonaromaticity, antiaromaticity,[8] or homoaromaticity and heteroaromaticity (as advocated by Schleyer et al.,[9] the structural "definition" of aromaticity is a "tendency toward bond length equalization and planarity (if applicable)"), of isomerization connected to N versus NH moieties, and the relation between the gas-phase acidity (or basicity) and the charge on nitrogen. Nevertheless, only few accurate r_e structure estimates are available for these heterocyclic molecules.[6,10−12] A list of references detailing work executed prior to 2007 can be found in ref 6. Though the situation improved since then, in an influential review published in 1980 Legon[13] noted that "in principle, it is possible to determine the equilibrium geometry (r_e), but sufficient data are as yet available in the case of no ring". A large number of accurate equilibrium structures are available for many other, simple(r) semirigid molecules,[14] but the situation is less than satisfactory for heterocyclic rings. One particular difficulty is that many heterocyclic rings are (nearly)

Special Issue: 25th Austin Symposium on Molecular Structure and Dynamics

Received: August 20, 2014
Revised: October 21, 2014

   dx.doi.org/10.1021/jp5084168 | *J. Phys. Chem. A* XXXX, XXX, XXX−XXX

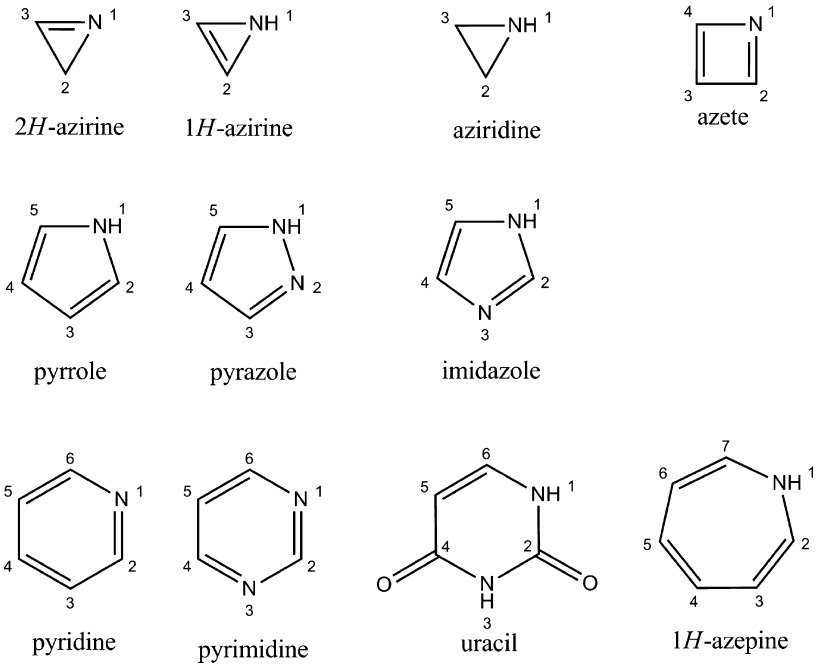

Figure 1. Schematic structures and atom numbering of the molecules investigated.

oblate tops. Molecules of this shape experience a large rotation of the principal axis system upon certain isotopic substitutions.[11] For such isotopologues it is difficult to obtain a good structural fit to the semiexperimental (SE) moments of inertia, I_a^{SE} and I_b^{SE}, which may significantly reduce the accuracy of the semiexperimental equilibrium structural parameters, r_e^{SE}. While some knowledge has been accumulated for the three-, four-, five-, six-, and seven-membered unsaturated heterocycles studied (see Figure 1), a firm grip on structural trends is provided first in this paper for several related systems. To keep focused, the literature results are discussed separately for each molecule investigated.

While some of the techniques that can be used to determine r_e estimates of molecular structures are discussed even in textbooks,[14] it is still highly beneficial to acquire further knowledge about the advantages and disadvantages of variants of these techniques (see Theoretical Background), especially for problematic cases. Thus, another goal of this work is to compare different methods, ab initio, semiexperimental, and empirical, to determine accurate equilibrium structures of medium-sized molecules.

2. THEORETICAL BACKGROUND

2.1. Born−Oppenheimer Equilibrium Structures. The highest level of electronic structure theory at which ab initio structures are optimized within this study is CCSD(T), the coupled cluster (CC) technique with single and double excitations[15] as well as a perturbative treatment of connected triples.[16] In the spirit of the focal-point analysis (FPA) technique,[17,18] the second-order Møller−Plesset (MP2) level[19] is also used extensively to estimate correction terms, whose computation at the CCSD(T) level seems unnecessarily expensive.

Different atom-centered, fixed-exponent Gaussian basis sets have been utilized during the optimizations, including the correlation-consistent basis sets cc-pVTZ and cc-pVQZ,[20] abbreviated throughout this paper as VTZ and VQZ, respectively. The augmented correlation-consistent basis set variants including diffuse functions, aug-cc-pVQZ and aug-cc-pV5Z,[21] abbreviated here as AVQZ and AV5Z, respectively, were also employed. Optimizations were also performed with the correlation-consistent polarized weighted core−valence triple-ζ, cc-pwCVTZ, and quadruple-ζ, cc-pwCVQZ, basis sets,[22,23] denoted here as wCVTZ, and wCVQZ, respectively. With the wCVTZ and wCVQZ basis sets all of the electrons were correlated (AE), whereas with the VTZ, VQZ, AVQZ, and AV5Z basis sets the frozen core (FC) approximation is normally used in correlated-level computations.

Different schemes were employed to determine the best estimates of the Born−Oppenheimer equilibrium structure, r_e^{BO}, of the molecules investigated. First, when possible, that is, for molecules not too large, the wCVQZ basis set was used and all electrons were correlated; consequently,

$$r_e^{BO}(\mathrm{I}) = \mathrm{CCSD(T)\_AE/wCVQZ} \quad (1)$$

The r_e^{BO} structure was also estimated in the FC approximation using the VQZ basis set and the CCSD(T) method. The core−core and core−valence correlation is missing from the CCSD(T)_FC/VQZ treatment; the corresponding structural corrections[24] were computed at the MP2 level using the wCVQZ basis set, resulting in another r_e^{BO} estimate:

$$r_e^{BO}(\mathrm{II}) = \mathrm{CCSD(T)\_FC/VQZ} + \mathrm{MP2(AE)/wCVQZ} - \mathrm{MP2(FC)/wCVQZ} \quad (2)$$

To check whether convergence is achieved at this level, the effect of further basis set enlargement was occasionally computed at the MP2 level using the AVQZ and AV5Z basis sets.

A third scheme was also utilized. For larger molecules, the structure was computed with the smaller wCVTZ basis set and the CCSD(T)_AE method, and the effect of further basis set enlargement, wCVTZ → wCVQZ, was estimated at the MP2

dx.doi.org/10.1021/jp5084168 | J. Phys. Chem. A XXXX, XXX, XXX−XXX

level. In other words, the r_e^{BO} parameters are obtained using the following equation:

$$r_e^{BO}(III) = CCSD(T)\_AE/wCVTZ + MP2(AE)/wCVQZ - MP2(AE)/wCVTZ \quad (3)$$

The basic assumption of eq 3 is that the correction due to basis set enlargement, wCVTZ → wCVQZ, is small and can, therefore, be estimated at the MP2 level. This approximation was investigated in several previous studies by us[4,11,82] and was found to be reliable. The approximation was further checked in the present work. For the smallest molecules, each of the three schemes were used, and the results were compared.

The CCSD(T) optimizations were performed with the CFOUR program package,[25] while the MP2 optimizations utilized the Gaussian09 suite of codes.[26]

2.2. Semiexperimental Equilibrium Structures. While the semiexperimental method has been employed in many studies and by many authors (see ref 14 for details), it is worth pointing out here that the fundamentals of this technique, yielding an r_e^{SE} equilibrium structure, were laid down in 1978 in ref 27. This paper is considered by many as a pioneering and significant contribution to structural chemistry by Peter Pulay, Wilfried Meyer, and Jim Boggs, not reflected correctly even by the close to 150 citations this paper received up to 2014.

To determine the semiexperimental equilibrium rotational constants, the published experimental ground-state rotational constants were employed first. However, as in the case of benzonitrile and phenylacetylene,[4] it became obvious that some of the fitted experimental rotational constants are not accurate enough for our purposes. For this reason, we redid the spectral fits in the same way as in refs 4 and 28: using the method of predicate observations, in which theoretical centrifugal distortion constants, derived from a quadratic B3LYP/6-311+G(3df,2pd) force field, are used as supplementary data in a weighted least-squares fit to the measured transitions.[29,30]

To correct the effective experimental rotational constants for each isotopologue and to obtain their equilibrium counterparts, cubic force field computations[31] were performed at the optimized structures with two different methods: (i) the Kohn−Sham density functional theory (DFT)[32] using Becke's three-parameter hybrid exchange functional[33] and the Lee−Yang−Parr correlation functional,[34] together denoted as B3LYP, with the 6-311+G(3df,2pd) basis set, and (ii) the MP2(FC) method with the standard VTZ basis. For pyrrole, the all-electron MP2 method was also used with the wCVTZ basis set. Although many DFT functionals could be used to compute anharmonic force fields, the B3LYP method was preferred as it is widely used and it provides accurate underlying equilibrium structures contributing to the fact that it is known to yield satisfactory force fields.[35,36] To avoid the nonzero force dilemma,[37] all force fields were evaluated at the corresponding optimized geometries. All anharmonic force field computations were performed with the electronic structure package Gaussian09.[26]

The semiexperimental equilibrium rotational constants, B_e^{SE}, were calculated from the experimental ground-state rotational constants, B_0, of the particular molecule using the equation

$$B_e^{SE} = B_0 + \Delta B_{vib} + \Delta B_{el} \quad (4)$$

where ΔB_{vib} is the rovibrational correction[38] calculated from the cubic force field, and ΔB_{el} is the electronic correction, which may be obtained from the rotational g tensor.[39]

The equilibrium structural parameters were determined by a weighted least-squares fit based on the semiexperimental equilibrium moments of inertia. The weights of the semiexperimental rotational constants were determined iteratively. At each step, an analysis of the residuals permitted checking the appropriateness of the weights and the compatibility of the rotational constants and the predicate observations. It is possible to automate, at least partly, this procedure by using the Iteratively Reweighted Least Squares (IRLS) method, whereby data with large residuals are weighted down.[29,40] Two weighting schemes are used: Huber weighting, where the weight linearly decreases as the residual increases, and biweight weighting, where, in addition, data with large residuals are eliminated.

When the number of isotopologues is not sufficient to calculate a structure, there is still another way to obtain an accurate structure estimate: extrapolating the computed ab initio rotational constants to infinite basis set size.[41,42] The ab initio equilibrium values of the rotational constants of the parent species X_e (X = A, B, C) are calculated first. For this, the ab initio structure was optimized using the CCSD(T) method with the cc-pwCVnZ basis sets (n = T, Q), with all electrons correlated. The rovibrational correction $\Delta X_0 = X_0 - X_e$ is added to these X_e(T) and X_e(Q) values, yielding X_0(T) and X_0(Q). The assumption that the ΔX_0 rovibrational corrections are almost constant, a generally excellent assumption,[43] is further verified here. Then, the rotational constants X_0(T) and X_0(Q) are extrapolated as a function of the computed structural parameters r_e(T) and r_e(Q). The intersection of the line with the experimental X_0 of the parent species gives the extrapolated r_e. With these r_e and the appropriate set of atomic masses the rotational constants of any missing isotopologue can be calculated, although with the increased computational effort described above.

2.3. Mass-Dependent Experimental Structures, r_m. In the particular case of oblate molecules it is often useful to determine the structure by the empirical mass-dependent method, r_m, proposed by Watson et al.[44] This technique takes into account the variation of the rovibrational correction upon isotopic substitution in an approximate manner. In particular, it takes care of the rotation of the principal axis system (PAS) and of the presence of small coordinates. In principle, it allows the determination of structures close to the assumed equilibrium structure.

In the PAS, $\xi = a, b, c$ of the parent isotopologue (i = 1), the three components of the ground-state moment of inertia of the parent are written as

$$I_\xi^0(1) = I_\xi^m + c_\xi\sqrt{I_\xi^m(1)} + d_\xi\hat{M}(1) \quad (5)$$

The last two terms of eq 5 provide the rovibrational contribution. $\hat{M}(1)$ is a known, coordinate-independent function of the atomic masses of a particular isotopologue, here of the parent (i = 1). This last term is useful when small Cartesian coordinates are present. In a center-of-mass coordinate system parallel to that of the parent, the elements of the 3 × 3 ground-state moment of inertia tensor of an isotopologue i must be written as

$$I_{\xi\eta}^0(i) = I_{\xi\eta}^m(i) + c_{\xi\eta}\sqrt{I_{\xi\eta}^m(i)} + \delta_{\xi\eta}d_\xi\cdot\hat{M}(i) \quad (6)$$

with rovibrational parameters $c_{\xi\eta}$ and d_ξ. Equation 6 defines elements of a nondiagonal 3 × 3 inertia tensor. The

dx.doi.org/10.1021/jp5084168 | J. Phys. Chem. A XXXX, XXX, XXX−XXX

nondiagonal terms $c_{\xi\eta}$ are useful when the rotation of the PAS upon isotopic substitution is large.

The model described above is named $r_m^{(2r)}$. When the nondiagonal terms $c_{\xi\eta}$ are neglected, we obtain the $r_m^{(2)}$ model. Setting $d_\xi = 0$ in eqs 5 and 6, the models $r_m^{(2r)}$ and $r_m^{(2)}$ reduce to models $r_m^{(1r)}$ and $r_m^{(1)}$, respectively. The accuracy is supposed to increase with the level of refinement of the model in the direction $r_m^{(1)} \rightarrow r_m^{(2r)}$. However, as the number of parameters to be fitted increases, the least-squares regression tends to become ill-conditioned, and the accuracy may actually get worse.

3. THREE-MEMBERED RINGS

The most stable form of the molecules with a C_2H_3N molecular formula and on the ground-state potential energy surface is methyl cyanide, CH_3CN. Next in the order of stability come 2*H*-azirine and ketenimine, $H_2C{=}C{=}NH$. The stability of 2*H*-azirine is increased by the electron-rich N atom. Nevertheless, the total ring-strain energy of 2*H*-azirine is substantial, on the order of 180 kJ mol^{-1}. 1*H*-azirine lies ∼170 kJ mol^{-1} above 2*H*-azirine.[45] The least stable form on the singlet C_2H_3N PES, iminocarbene, is predicted to be less stable than 1*H*-azirine by some 270 kJ mol^{-1}; in fact, this molecule has a triplet ground electronic state.

3.1. Structure of 2*H*-Azirine. 2*H*-azirine (often called 1-azirine, where the number refers to the position of the double bond), *c*-CH_2CHN, is a three-membered heterocyclic molecule with an equilibrium structure of C_s point-group symmetry, containing a nitrogen atom and a C=N double bond (see Figure 1).

The microwave (MW) spectrum of 2*H*-azirine was measured first in 1976 by Ford.[46] That study was later extended to the millimeterwave (MMW) range permitting the determination of accurate ground-state spectroscopic constants for the parent species.[47] While numerous ab initio computations have been performed on C_2H_3N species to determine the relative stability of the different structural isomers,[43] up to now no accurate equilibrium structures have been determined for the cyclic 1*H*- and 2*H*-azirine molecules.

The r_e^{BO} structure of 2*H*-azirine was estimated via eqs 1−3, and the results obtained are listed in Table 1. The three equations yield almost identical structural parameters. Furthermore, an attempt to improve the accuracy of the r_e^{BO} estimate by using the larger V5Z basis set and by taking into account the effect of diffuse functions by utilizing the AV5Z basis shows that these two effects almost fully compensate each other at the MP2 level and can thus be safely neglected even at the level of accuracy sought in this study.

As only the rotational constants of the parent species are known, it is not possible to determine an r_e^{SE} structure for this molecule. However, the extrapolation method described at the end of Section 2.2 can be utilized. This procedure was tried with the B3LYP/6-311+G(3df,2pd) anharmonic force field and was repeated for each rotational constant $X = A$, B, and C. The overall agreement between the r_e^{BO} and r_e^{SE} structures is extremely good, as can be seen in Table S1 of the Supporting Information, and the mean of the results is given in the last column of Table 1. What is even more convincing is that if we change the rovibrational corrections by 5%, the structural results do not change significantly, indicating that they are quite precise and accurate.

It is worth noting that the single $N_1{-}C_2$ bond of 2*H*-azirine at $r_e^{SE} = r_e^{BO}(I) = 1.546$ Å is substantially longer than the C−N bond in acyclic methylamine, CH_3NH_2, whose $r_e^{BO}(I)$ value is

Table 1. Equilibrium Structural Parameters of 2*H*-Azirine[a]

method	CCSD(T)	MP2	MP2	CCSD(T)	MP2	MP2	diff.[b]	CCSD(T)[c]	r_e^{BO}(II)[d]	r_e^{BO}(III)[e]	r_e^{SE}[f]
approx.[g]	FC	AE	FC	AE	AE	FC	FC	AE			
basis set	VQZ	wCVQZ	wCVQZ	wCVTZ	wCVTZ	VQZ	AV5Z	wCVQZ			
$N_1{=}C_3$	1.2575	1.2576	1.2609	1.2568	1.2598	1.2614	1.2610	−0.0004	1.2542	1.2542	1.2546	1.2546
$N_1{-}C_2$	1.5503	1.5481	1.553	1.5517	1.5534	1.5536	1.5530	−0.0006	1.5455	1.5454	1.5464	1.5463
$C_2{-}C_3$	1.4510	1.4399	1.4431	1.4496	1.4416	1.4435	1.4435	0.0000	1.4476	1.4478	1.4479	1.4479
$C_3{-}H$	1.0791	1.0754	1.0769	1.0786	1.0765	1.0769	1.0768	−0.0001	1.0776	1.0776	1.0775	1.0778
$C_2{-}H$	1.0824	1.0779	1.0794	1.0815	1.0787	1.0795	1.0794	−0.0001	1.0809	1.0809	1.0807	1.0809
∠(N_1C_3H)	139.04	138.92	138.88	139.08	138.92	138.88	138.83	−0.055	139.06	139.07	139.07	139.06
∠(C_2C_3H)	151.55	151.42	151.39	151.37	151.24	151.38	151.46	0.080	151.58	151.57	151.55	151.55
∠(N_1C_2H)	115.82	115.46	115.40	115.83	115.44	115.40	115.36	−0.043	115.87	115.88	115.85	115.86
∠(C_3C_2H)	120.40	120.38	120.37	120.44	120.40	120.37	120.33	−0.037	120.42	120.41	120.41	120.42
∠(HC_2H)	116.65	116.91	116.96	116.61	116.89	116.97	117.05	0.086	116.59	116.61	116.62	116.59
$H_3C_3C_2H_2$	−80.66	−81.05	−81.13	−80.69	−81.11	−81.13	−81.16	−0.032	−80.61	−80.59	−80.63	−80.62

[a]Distances in Å and angles in degrees. [b]MP2(FC)/AV5Z − MP2(FC)/VQZ. [c]r_e^{BO}(I), see eq 1. [d]See eq 2. [e]See eq 3. [f]See text and Table S1 of the Supporting Information. [g]AE = all electrons correlated; FC = frozen core approximation.

dx.doi.org/10.1021/jp5084168 | J. Phys. Chem. A XXXX, XXX, XXX−XXX

Table 2. Equilibrium Structural Parameters of 1*H*-Azirine[a]

parameter	FC-CCSD(T)[b] VQZ	AE-CCSD(T)[b] wCVQZ	FC-CCSD(T)[b,c] wCVQZ	r_e^{BO}(II)[d]
NC	1.5219	1.5174	1.5214	1.5179
NH	1.0233	1.0221	1.0234	1.0220
C=C	1.2794	1.2762	1.2789	1.2767
CH	1.0716	1.0702	1.0715	1.0703
∠(CNH)	106.64	106.80	106.67	106.78
∠(NCH)	138.11	138.17	138.13	138.15
∠(CCH)	156.74	156.70	156.73	156.71
HNCH	82.04	81.95	82.03	81.97

[a]Distances in Å and angles in degrees. [b]AE = all electrons correlated; FC = frozen core approximation. [c]r_e^{BO}(I), see eq 1. [d]See eq 2.

Table 3. Structure of Aziridine[a]

parameter[b]	r_e^{BO} [c]	MP2/VQZ[d]	MP2/AV5Z[d]	r_e^{BO} [e]	r_e^{SE}	$r_m^{(2)}$	r_s [f]
CN	1.47024	1.4702	1.4703	1.4703	1.47013(6)	1.4698(7)	1.475
CC	1.47736	1.4758	1.4756	1.4772	1.47703(8)	1.4771(9)	1.481
NH	1.01244	1.0124	1.0124	1.0124	1.01279(13)	1.0133(4)	1.016
CH_c	1.08082	1.0794	1.0793	1.0807	1.08099(13)	1.0821(3)	1.084
CH_t	1.07956	1.0781	1.0780	1.0795	1.07971(13)	1.0810(3)	1.083
∠(HNC)	109.17	109.00	109.20	109.37	109.376(9)	109.38(3)	
∠(CNC)	60.32	60.25	60.24	60.31	60.311(6)	60.33(3)	60.25
∠(NCC)	59.84	59.87	59.88	59.85	59.845(3)	59.84(2)	
∠(H_cCH_t)	115.33	115.60	115.69	115.42	115.424(9)	115.59(8)	115.72
∠(NCH_c)	118.35	118.32	118.23	118.26	118.28(2)	118.34(7)	118.26
∠(NCH_t)	114.51	114.31	114.24	114.44	114.46(2)	114.32(7)	114.27
∠(CCH_c)	117.82	117.68	117.71	117.85	117.829(14)	117.80(4)	117.75
∠(CCH_t)	119.59	119.50	119.46	119.55	119.538(14)	119.37(5)	119.32

[a]Distances in Å and angles in degrees. [b]The carbon-bonded cis hydrogens (subscript c) are situated on the same side of the plane of the triangle C−N−C as the nitrogen-bonded hydrogen. [c]r_e^{BO}(I), corresponding to an all-electron CCSD(T)/cc-pwCVQZ optimization. [d]Frozen core approximation. [e]Correction MP2(FC)/AV5Z −MP2(FC)/VQZ included. [f]Reference 52.

1.461 Å. Furthermore, the C_2-C_3 bond, at 1.448 Å, is substantially shorter than it is in acyclic molecules. These structural results are in clear agreement with the antiaromatic nature of 2*H*-azirine. The long C_2-N bond is also consistent with the major thermal reaction of 2*H*-azirines, as via cleavage of this bond one can form vinyl nitrene intermediates from them.

3.2. Structure of 1*H*-Azirine. 2*H*-azirine, whose equilibrium structure was determined in the previous section, has been computed[43] to be considerably more stable than its tautomeric form 1*H*-azirine (2-azirine using the other common nomenclature): 1*H*-azirine is inherently antiaromatic (its planar form would have four π electrons), its ring strain is substantial, and thus the molecule has high reactivity.

Since the 1*H*-azirine molecule is rather unstable, no experimental results concerning its MW and MMW spectra are available. Nevertheless, an accurate r_e^{BO} structure can be computed for this simple triatomic heterocycle. The r_e^{BO} structure of 1*H*-azirine was estimated via eqs 1 and 2; however, for the latter equation the core correlation was computed at the CCSD(T) level. The results obtained are listed in Table 2. Just like 2*H*-azirine, 1*H*-azirine has a very long NC (1.518 Å) and a short C=C (1.277 Å) bond. To relieve strain due to antiaromaticity, the NH structural unit of 1*H*-azirine is strongly out of the plane defined by the three heavy atoms.

3.3. Structure of Aziridine. Aziridine, *c*-C_2H_4NH, also called ethylene imine, is a nonaromatic three-membered saturated N-heterocycle. It is the only saturated N-heterocycle whose equilibrium structure is investigated in this study. Aziridine is the saturated equivalent of 1*H*-azirine, and it is the nitrogen analogue of epoxide.

The equilibrium structure of aziridine exhibits C_s point-group symmetry. The barrier for the pyramidal inversion around N is large, some 80 kJ mol^{-1}, while the ring-strain energy of aziridine is similar to that of cyclopropane, about 110 kJ mol^{-1}. The rotational spectrum of aziridine has been studied in great detail, see refs 48−50 for a review of earlier work. It is a molecule worth studying in detail because of its potential astrophysical interest.[48] Furthermore, it is an oblate top (Ray's asymmetry parameter, κ = +0.67) not too far from the spherical top limit, making its centrifugal distortion analysis and the determination of its structure particularly interesting. Its infrared spectrum was recently recorded at high resolution and analyzed.[51] Particularly relevant to the present study is the work of Bak and Skaarup,[52] who measured the spectra of the monoisotopically substituted species and who determined a complete substitution structure, r_s, for this molecule.

The r_e^{BO}(I) structural parameters of aziridine are reported in Table 3. An attempt to improve the accuracy of the r_e^{BO} estimate by using the larger V5Z basis set and by taking into account the effect of diffuse functions via utilizing the AV5Z basis shows that these two effects almost fully compensate each other at the MP2 level, except for the ∠(HNC) bond angle, which increases by 0.2° when going from MP2(FC)/VQZ to MP2/(FC)/AV5Z. For this particular structural parameter, the increase is due both to the diffuse functions and to the larger V5Z basis set, the increase being 0.14° when going from MP2(FC)/VQZ to MP2(FC)/AVQZ.

dx.doi.org/10.1021/jp5084168 | J. Phys. Chem. A XXXX, XXX, XXX−XXX

Table 4. Structure of Azete[a]

method	CCSD(T)	MP2	MP2	CCSD(T)	MP2	MP2	MP2	diff.[b]	CCSD(T)[c]	r_e^{BO}(II)[d]	r_e^{BO}(III)[e]
approx.[f]	FC	AE	FC	AE	AE	FC	FC		AE		
basis set	VQZ	wCVQZ	wCVQZ	wCVTZ	wCVTZ	VQZ	AV5Z		wCVQZ		
N_1-C_2	1.2913	1.2847	1.2877	1.2908	1.2865	1.2881	1.2881	0.0000	1.2882	1.2883	1.2890
C_2-C_3	1.5454	1.5354	1.5388	1.5440	1.5377	1.5393	1.5385	−0.0008	1.5419	1.5420	1.5417
C_3-C_4	1.3397	1.3291	1.3324	1.3386	1.331	1.3329	1.3325	−0.0004	1.3362	1.3364	1.3367
N_1-C_4	1.5549	1.5558	1.5598	1.5569	1.5612	1.5604	1.5593	−0.0011	1.5509	1.5509	1.5515
C_2-H_2	1.0846	1.0816	1.0831	1.0839	1.0825	1.0832	1.0831	−0.0001	1.0831	1.0831	1.0830
C_3-H_3	1.0786	1.0756	1.0772	1.0781	1.0767	1.0772	1.0772	0.0000	1.0771	1.0770	1.0770
C_4-H_4	1.0791	1.0759	1.0774	1.0785	1.0768	1.0774	1.0774	0.0000	1.0776	1.0776	1.0776
$\angle N_1C_2C_3$	96.05	96.38	96.42	96.16	96.52	96.43	96.36	−0.06	96.01	96.07	96.02
$\angle C_2C_3C_4$	84.54	84.69	84.67	84.58	84.69	84.67	84.72	0.05	84.56	84.57	84.58
$\angle C_3C_2H_2$	136.62	136.25	136.23	136.50	136.11	136.22	136.31	0.09	136.63	136.61	136.64
$\angle C_2C_3H_3$	138.59	138.97	138.98	138.59	138.99	138.97	138.95	−0.02	138.60	138.55	138.57
$\angle H_4C_4C_3$	139.14	139.59	139.63	139.13	139.61	139.65	139.68	0.03	139.11	139.17	139.11

[a]Distances in Å and angles in degrees. [b]MP2(FC)/AV5Z − MP2(FC)/VQZ. [c]r_e^{BO}(I), see eq 1. [d]See eq 2. [e]See eq 3. [f]AE = all electrons correlated; FC = frozen core approximation.

The anharmonic force fields of the eight isotopologues for which measured rotational constants are available were computed at the MP2(FC)/VTZ level of electronic structure theory. The derived α-constants were combined with the experimental ground-state rotational constants to yield estimates of semiexperimental equilibrium rotational constants, which were also corrected for the electronic contribution. The experimental ground state and semiexperimental equilibrium rotational constants are given in Table S2 of the Supporting Information. The experimental values of the molecular g-tensor are taken from ref 53. The semiexperimental equilibrium structure is determined by a weighted least-squares fit using an uncertainty of 0.2 MHz for A and B and 0.1 MHz for C. The fit is extremely well-conditioned, indicating that the derived structure is likely to be reliable. This r_e^{SE} structure is given in Table 3 and can be compared to the r_e^{BO} estimate. The agreement is almost perfect. Inspection of the residuals of the fit, also given in Supporting Information, Table S2, shows that there are a few large residuals, in particular for the A and B constants of the c-C_2H_4ND species. These disagreements may be explained by the fact that the angle of rotation of the PAS upon substitution is very large, φ = 177°, and further confirmed by the large residuals of the A and B rotational constants, which have about the same absolute value but of opposite sign. However, these difficulties do not significantly affect the quality of the fit. The r_s and the empirical $r_m^{(2)}$ structures are also given in Table 3. It is interesting to note that the empirical $r_m^{(2)}$ structure is in surprisingly good agreement with the equilibrium structures. This may be explained by the favorable conditioning of the least-squares system.

The structure of aziridine is close to those of cyclopropane[54] and oxirane.[11] The ∠CNC angle at 60.3° is close to the ∠CCC angle in cyclopropane, 60°, and considerably smaller than the analogous ∠COC angle in oxirane, 61.9°. The CC bond length in aziridine at 1.477 Å is intermediate between the values found in cyclopropane, 1.504 Å, and in oxirane, 1.461 Å. This indicates a steady increase of the double bond character when going from cyclopropane to oxirane through aziridine. The ∠HCH angle in aziridine at 115.4° is also intermediate between the values found in cyclopropane, 114.8°, and in oxirane, 116.1°. Likewise, the CH bond length in aziridine at ∼1.080−1.081 Å is also intermediate between the values found in cyclopropane, 1.079 Å, and in oxirane, 1.082 Å. As a consequence, the nonbonded d(H···H) distance is not constant in these molecules.

4. FOUR-MEMBERED RINGS: AZETE

Azete, c-C_3H_3N, is an unsaturated four-membered ring with three carbon atoms, one nitrogen atom, and two formal double bonds (Figure 1). It is extremely unstable, as would follow immediately from its alternate name azacyclobutadiene and its molecular orbital level structure. Azete has conjugated double bonds that form a system of four π-electrons. Therefore, it behaves as an extremely reactive diradical. The MW spectrum of azete has not yet been analyzed.

The r_e^{BO} structure of azete was determined using eqs 1−3, and the results are presented in Table 4. As for 2H-azirine, these three equations give almost identical results. Furthermore, an attempt to improve the accuracy of the r_e^{BO} estimate by using the larger V5Z basis set and by taking into account the effect of diffuse functions at the AV5Z level shows that these two effects almost compensate each other and can thus be neglected.

It is interesting to note that the length of the single bond N_1-C_4 at 1.551 Å is significantly longer than the C−N bond length in methylamine, CH_3NH_2, whose corresponding r_e^{BO}(I) value is 1.461 Å. This is in agreement with the pronounced antiaromatic nature of azete.

5. FIVE-MEMBERED RINGS

The MW spectra of the five-membered N-heterocycles investigated here, namely, pyrrole, pyrazole, and imidazole (Figure 1), have all been investigated experimentally. Therefore, for these molecules not only r_e^{BO} but also dependable r_e^{SE} structures can be determined.

5.1. Structure of Pyrrole. Pyrrole is a nonbasic N-heterocyclic aromatic compound of formula C_4H_4NH. It is a planar five-membered ring with an equilibrium structure of point-group symmetry C_{2v} (Figure 1).

The MW spectrum of this oblate molecule (κ = +0.94) and its six monosubstituted isotopic species was studied by Nygaard et al.,[55] and a substitution structure was derived. More recently, the MMW spectrum of the parent species was measured.[56] The ground-state rotational constants were further improved by a combined fit of rotational transitions and ground-state combination differences.[57] The analysis of the vibrational

dx.doi.org/10.1021/jp5084168 | J. Phys. Chem. A XXXX, XXX, XXX−XXX

Table 5. Structure of Pyrrole[a]

method	MP2(AE)		CCSD(T)	r_e^{BO} [b]	r_e^{SE}		$r_m^{(1)}$	r_s [c]
basis set	CVTZ	wCVQZ	CVTZ AE		B3LYP[d]	MP2[e]		
CN	1.3653	1.3628	1.37173	1.3692	1.3694(2)	1.36940(17)	1.3764(10)	1.370
NH	1.0027	1.0022	1.00175	1.0013	1.00062(17)	1.00086(14)	0.9943(8)	0.996
C_2C_3	1.3787	1.3760	1.37625	1.3736	1.3728(3)	1.3723(2)	1.3783(15)	1.382
C_2H	1.0742	1.0731	1.07589	1.0748	1.07452(15)	1.07532(13)	1.0740(8)	1.076
C_3C_4	1.4130	1.4105	1.42502	1.4225	1.4232(5)	1.4231(4)	1.430(3)	1.417
C_3H	1.0749	1.0738	1.07667	1.0756	1.07436(17)	1.07527(16)	1.0747(9)	1.077
∠CNC	110.18	110.19	109.81	109.82	109.82(2)	109.809(16)	109.67(9)	109.8
∠CNH	124.91	124.90	125.10	125.09	125.089(10)	125.096(8)	125.16(5)	121.5
$\angle NC_2C_3$	107.48	107.46	107.77	107.76	107.76(2)	107.762(15)	107.85(9)	107.7
$\angle NC_2H$	121.31	121.32	121.18	121.19	121.04(9)	120.99(7)	121.5(5)	
$\angle C_3C_2H$	131.22	131.21	131.05	131.05	131.20(9)	131.25(7)	130.7(5)	
$\angle C_2C_3C_4$	107.43	107.44	107.33	107.33	107.329(13)	107.334(12)	107.32(7)	107.4
$\angle C_2C_3H$	125.50	125.50	125.70	125.70	125.98(9)	125.94(6)	126.0(5)	
$\angle C_4C_3H$	127.06	127.06	126.98	126.97	126.69(8)	126.73(5)	126.6(5)	127.1

[a]Distances in Å and angles in degrees. [b]From eq 3. [c]Reference 55. [d]Rovibrational corrections from the B3LYP/6-311+G(3df,2pd) cubic force field. [e]Rovibrational corrections from the MP2(AE)/wCVTZ cubic force field.

spectrum has been reviewed by Hegelund et al.[58] These authors also computed ab initio the rotational, centrifugal distortion, and vibration−rotation interaction constants.[59] There is also a determination of the structure of pyrrole-^{15}N in nematic liquid crystals.[60] However, a complex formation was observed between pyrrole and the liquid-crystal molecules hampering an accurate structure determination. Finally, note that the electronic spectrum of pyrrole has been investigated by using a hierarchy of coupled-cluster methods.[61]

An estimate to r_e^{BO} of pyrrole was computed using eq 3. The structural parameters obtained are given in Table 5.

To determine r_e^{SE} of pyrrole, two cubic force fields were computed, at the B3LYP/6-311+G(3df,2pd) and MP2(AE)/wCVTZ levels of theory. The ground-state rotational constants of the parent species were taken from ref 56. The ground-state rotational spectra of the isotopic species were refitted using as predicates the quartic centrifugal distortion constants derived from the harmonic force field computed at the B3LYP/6-311+G(3df,2pd) level of theory. The experimental frequencies were taken from ref 55. The experimental values of the molecular g-tensor are taken from ref 53. The experimental ground-state and semiexperimental equilibrium rotational constants, obtained with the help of a MP2(AE)/wCVTZ cubic force field, as well as the inertial defects, are given in Table S3 of the Supporting Information.

The semiexperimental structure, given in Table 5, is determined by an iteratively reweighted least-squares fit using the biweight weighting scheme. The r_e^{SE} structures derived with the MP2 and B3LYP force fields are in good agreement with the r_e^{BO} structure; the largest differences can be observed for the ∠CCH angles, up to 0.2° for $\angle C_2C_3H$. The r_e^{SE} structure derived from the B3LYP/6-311+G(3df,2pd) cubic force field is marginally less accurate, but the difference may be considered negligible. To estimate the quality of the derived structure, it is informative to have a look at the equilibrium inertial defect, which should be exactly zero for a planar molecule. The experimental ground-state inertial defect is Δ_0 = +0.0162 uÅ^2 for the parent species; after the rovibrational correction, based on the MP2/wCVTZ force field, it becomes −0.0087 uÅ^2, and after the electronic correction it is Δ_e = 0.0004 uÅ^2, that is, practically zero. This confirms that the rovibrational correction is likely to be accurate and that the electronic correction, although small, is not negligible. The B3LYP/6-311+G(3df,2pd) force field gives similar results, Δ_e = −0.0007 uÅ^2 after inclusion of the electronic correction. Similar values are obtained for the isotopic species; however, the values for the deuterated species are slightly worse, in particular for the ND species. This observation may be because the ground-state rotational constants of this isotopologue are less accurate, but it could also be explained by a small deficiency of the force field. This is confirmed by the fact that the residual for the A constant of the ND species, shown in Supporting Information, Table S3, is large. The angle of rotation of the PAS upon isotopic substitution, also shown in Supporting Information, Table S3, is large; in particular, there is an a/b axis switching from the $^{13}C_2$ and D_2 species. However, this switching does not seem to affect the quality of the fit. This stability is probably the consequence of the good conditioning of the fit: thanks to the C_{2v} point-group symmetry, the number of parameters to be determined is small, compared to the number of independent rotational constants, 14.

As expected, the structure of pyrrole is close to that of furane.[11] Nevertheless, there are a couple of noteworthy differences. The C_2C_3 bond in pyrrole at 1.374 Å is slightly longer than that in furane, 1.355 Å, while the C_3C_4 bond at 1.423 Å is slightly shorter than in furane, 1.434 Å. Furthermore, $\angle C_2C_3C_4$ at 107.3° in pyrrole is slightly larger than it is in furane, where it is 106°. Also as expected, the differences between the equilibrium structures of pyrrole and cyclopentadiene[62] are significant: the geometrical parameters for this last molecule are C_2C_3 = 1.346 Å, C_3C_4 = 1.466 Å, and $\angle C_2C_3C_4$ = 109.13°.

5.2. Structure of Pyrazole. Pyrazole is a planar, near-oblate (κ = +0.915) N-heterocyclic aromatic compound with the formula $C_3H_3N_2H$ (Figure 1). It is a five-membered ring with two adjacent nitrogen atoms. The derivatives of pyrazole have many medicinal applications.

The MW spectrum of pyrazole was first measured by Kirchhoff.[63] Later, Nygaard et al.[64] have investigated the MW spectra of the complete set of monosubstituted isotopic pyrazoles and have determined a complete r_s structure. The rotational Zeeman spectrum of the parent species has been studied by Stolze and Sutter.[65] The rotational spectrum of 1-D-pyrazole was studied by microwave Fourier transform

dx.doi.org/10.1021/jp5084168 | J. Phys. Chem. A XXXX, XXX, XXX−XXX

Table 6. Structure of Pyrazole[a]

method	MP2(AE)		CCSD(T) AE	r_e^{BO} [b]	r_e^{SE}	$r_m^{(1)}$	r_s [c]
basis set	CVTZ	wCVQZ	CVTZ				
N_1-H	1.0040	1.0034	1.0025	1.0020	1.0014(4)	0.9956(4)	0.9978(4)
N_1-N_2	1.3362	1.3334	1.3465	1.3437	1.3431(6)	1.348(1)	1.3488(6)
$N_2=C_3$	1.3407	1.3378	1.3323	1.3293	1.3286(7)	1.329(1)	1.3306(5)
N_1-C_5	1.3528	1.3500	1.3547	1.3518	1.3523(6)	1.354(1)	1.3591(1)
C_3-C_4	1.4005	1.3979	1.4122	1.4096	1.4093(6)	1.411(1)	1.4162(2)
$C_4=C_5$	1.3802	1.3774	1.3792	1.3765	1.3771(8)	1.376(1)	1.3724(4)
C_3-H	1.0749	1.0739	1.0770	1.0759	1.0755(4)	1.0763(4)	1.0784(4)
C_4-H	1.0736	1.0725	1.0752	1.0741	1.0736(4)	1.0738(4)	1.0756(5)
C_5-H	1.0743	1.0732	1.0761	1.0750	1.0740(5)	1.0751(4)	1.0774(5)
$\angle HN_1N_2$	118.69	118.74	118.92	118.97	118.97(11)	118.61(12)	118.40(3)
$\angle HN_1C_5$	127.47	127.52	127.70	127.75	127.79(12)	128.32(13)	
$\angle N_2N_1C_5$	113.84	113.74	113.38	113.28	113.24(5)	113.07(5)	113.07(3)
$\angle N_1N_2C_3$	103.74	103.89	103.93	104.08	104.18(3)	104.12(4)	104.07(1)
$\angle N_1C_5C_4$	105.80	105.83	106.24	106.27	106.23(4)	106.36(4)	106.42(2)
$\angle N_1C_5H$	121.90	121.89	121.78	121.77	121.84(11)	121.47(10)	121.47(4)
$\angle C_4C_5H$	132.30	132.28	131.98	131.96	131.93(10)	132.16(9)	
$\angle N_2C_3C_4$	111.88	111.75	112.07	111.94	111.90(5)	111.97(5)	111.94(3)
$\angle N_2C_3H$	119.21	119.26	119.41	119.46	119.49(14)	119.59(14)	119.31(4)
$\angle C_4C_3H$	128.91	128.99	128.53	128.60	128.62(15)	128.44(15)	
$\angle C_5C_4C_3$	104.74	104.80	104.38	104.43	104.46(4)	104.48(3)	104.50(2)
$\angle C_5C_4H$	126.95	126.93	127.29	127.27	127.23(13)	127.67(11)	
$\angle C_3C_4H$	128.31	128.27	128.33	128.30	128.32(13)	127.85(12)	127.90(5)

[a]Distances in Å and angles in degrees. [b]From eq 1. [c]Reference 64.

Table 7. Structure of Imidazole[a]

	CCSD(T)	MP2 (AE)		r_e^{BO} [b]	r_e^{SE} [c]	$r_m^{(2r)}$	r_e^{SE} [d]	r_s [e]
	CVTZ AE	CVTZ	wCVQZ					
N_1-C_2	1.36216	1.3586	1.3561	1.3597	1.3612(9)	1.3612(10)	1.3594(3)	1.369
N_1-C_5	1.3774	1.3678	1.3652	1.3748	1.3738(9)	1.3735(10)	1.3758(3)	1.3777
N_1-H	1.00316	1.0038	1.0033	1.0027	1.0008(5)	0.9952(4)	1.0013(1)	0.995
$C_2=N_3$	1.3140	1.3182	1.3154	1.3112	1.3111(8)	1.3093(8)	1.3114(2)	1.3164
C_2-H	1.07731	1.0749	1.0738	1.0762	1.0759(6)	1.0769(4)	1.0761(1)	1.075
N_3-C_4	1.38035	1.3692	1.3663	1.3775	1.3797(8)	1.3788(9)	1.3774(3)	1.388
$C_4=C_5$	1.36952	1.3729	1.3702	1.3668	1.3627(8)	1.3605(9)	1.3663(3)	1.3672
C_4-H	1.07658	1.0746	1.0735	1.0755	1.0747(6)	1.0756(4)	1.0749(2)	1.0733
C_5-H	1.07522	1.0733	1.0722	1.0741	1.0764(5)	1.0763(4)	1.0734(3)	1.0766
$\angle C_2N_1C_5$	107.17	107.58	107.63	107.22	107.02(5)	106.90(4)	107.18(1)	106.96
$\angle C_2N_1H_1$	126.42	126.24	126.20	126.38	126.23(16)	126.27(11)	126.44(4)	
$\angle C_5N_1H_1$	126.42	126.18	126.17	126.40	126.75(15)	126.83(11)	126.38(3)	
$\angle N_1C_2N_3$	112.01	111.56	111.41	111.87	111.91(6)	111.97(4)	111.90(2)	111.87
$\angle N_1C_2H_2$	122.25	122.45	122.53	122.32	122.53(12)	122.44(9)	122.39(3)	
$\angle N_3C_2H_2$	125.74	126.00	126.06	125.81	125.57(12)	125.59(9)	125.71(3)	
$\angle C_2N_3C_4$	104.92	105.07	105.25	105.10	105.02(5)	104.99(4)	105.08(2)	105.04
$\angle N_3C_4C_5$	110.78	110.82	110.69	110.66	110.60(6)	110.64(4)	110.69(2)	110.45
$\angle N_3C_4H_4$	121.39	121.56	121.61	121.43	121.51(11)	121.46(8)	121.48(3)	
$\angle C_5C_4H_4$	127.83	127.62	127.70	127.91	127.89(11)	127.90(8)	127.83(4)	
$\angle N_1C_5C_4$	105.12	104.98	105.02	105.16	105.45(6)	105.50(4)	105.16(3)	105.68
$\angle N_1C_5H_5$	122.27	122.40	122.40	122.27	121.92(12)	121.95(9)	122.29(3)	
$\angle C_4C_5H_5$	132.61	132.62	132.57	132.57	132.62(12)	132.55(9)	132.56(4)	

[a]Distances in Å and angles in degrees. [b]From eq 1. [c]Simple weighted fit. [d]Fit with predicates, see text. [e]Reference 70.

(MWFT) spectroscopy and by Zeeman spectroscopy by Böttcher and Sutter.[66] The MMW spectrum of the parent species was measured, and a complete ab initio quadratic force field was calculated by Wlodaraczak et al.[67] There are also ab initio estimates of the equilibrium structure of pyrazole determined by electronic structure computations up to the QCISD level of theory.[68]

In the present study, an estimate to r_e^{BO} of pyrazole was computed using eq 3. The structural results obtained are given in Table 6.

To determine the semiexperimental structure, the cubic force field was computed at the B3LYP/6-311+G(3df,2pd) level of theory. The derived α-constants were combined with the experimental ground-state rotational constants to yield

dx.doi.org/10.1021/jp5084168 | J. Phys. Chem. A XXXX, XXX, XXX−XXX

estimates of semiexperimental equilibrium rotational constants, which were also corrected for the electronic contribution. The experimental values of the molecular *g*-tensor were taken from refs 65 and 66. The experimental ground-state inertial defect is $\Delta_0 = +0.0316$ uÅ^2 for the parent species; after the rovibrational correction it becomes −0.0104 uÅ^2, and after the electronic correction it is $\Delta_e = -0.0007$ uÅ^2, that is, practically zero. This confirms that the rovibrational correction is likely to be accurate and that the electronic correction, although small, is once more not negligible. Similar values to those reported above are obtained for the isotopic species, with a very narrow range of 0.0008 uÅ^2 for the equilibrium inertial defect. The ground-state and semiexperimental equilibrium rotational constants are given in Table S4 of the Supporting Information.

A weighted structural fit employing uncertainties of 0.05 MHz for A_e and B_e and 0.02 MHz for C_e provides satisfactory results. The derived structural parameters are given in Table 6, and the residuals of the fit are given in Table S4 of the Supporting Information. Inspection of these residuals shows that for the species $^{15}N_1$ and $^{13}C_3$ the values are large for *A* and *B* and of opposite sign, which is typical of an oblate molecule with large rotation of the PAS upon isotopic substitution.[11] However, the standard deviations of the structural parameters remain small, and it is also telling that the r_e^{SE} structure is in very good agreement with the r_e^{BO} one.

The r_s and the empirical $r_m^{(1)}$ structures are also given in Table 6. It is interesting to note that the empirical $r_m^{(1)}$ structure is in fair agreement with the equilibrium structure.

5.3. Structure of Imidazole. Imidazole is a structural isomer of pyrazole with two nonadjacent nitrogen atoms. It exists in two equivalent tautomeric forms, and the molecule is amphoteric: the N_1−H group is a proton donor, and the N_3 atom is a proton acceptor. Imidazole is incorporated in many biological molecules, for instance, histidine. Its equilibrium structure on the ground electronic state has C_s point-group symmetry, and the molecule is an oblate top with $\kappa = +0.86$.

The MW spectrum of imidazole was first analyzed by Blackman et al.,[69] who paid attention to the complex quadrupole hyperfine splitting. Christen et al.[70] measured the MW spectra of 11 isotopic species, including single substitution for each atom, and they determined a complete r_s structure of imidazole.

The best estimate to r_e^{BO} of imidazole was computed using eq 3, with structural parameters given in Table 7. Addition of diffuse functions to the wCVQZ basis set (aug-cc-pwCVQZ) has a very small effect on the structure: the CN bond lengths are lengthened by less than 0.0007 Å, this lengthening being partly compensated by enlargement of the basis from wCVQZ to wCV5Z, while the effect on the angles is also smaller than 0.07°.

To improve the quality of the rotational constants employed during the structural fit, the ground-state rotational spectra of all species were refitted using as predicates the quartic centrifugal distortion constants derived from the harmonic force field computed at the B3LYP/6-311+G(3df,2pd) level. The experimental rotational frequencies were taken from ref 70. The anharmonic force fields of the 11 isotopologues were computed at the B3LYP/6-311+G(3df,2pd) level. The derived α-constants were combined with the experimental ground-state rotational constants to yield estimates of semiexperimental equilibrium rotational constants, which were also corrected for the electronic contribution. The experimental values of the molecular *g*-tensor were taken from ref 65. The ground-state and semiexperimental equilibrium rotational constants, as well as the inertial defects, are given in Table S5 of the Supporting Information. The experimental ground-state inertial defect is $\Delta_0 = +0.0287$ uÅ^2 for the parent species; after the rovibrational correction it becomes −0.0107 uÅ^2, and after the electronic correction it is $\Delta_e = -0.0016$ uÅ^2, that is, practically zero. Similar results are obtained for the isotopic species. This indicates that the rovibrational corrections are probably accurate and that the electronic correction, although small, is not negligible, as found repeatedly in this study.

The r_e^{SE} structure of imidazole was first determined by a weighted least-squares fit. The structural parameters obtained, given in Table 7, especially those related to C_5, are not satisfactory; the r_e^{SE} value for the C_4−C_5 bond length is too short by 0.004 Å, and the $\angle N_1C_5C_4$ and $\angle N_1C_5H_5$ angles deviate by 0.3° from their r_e^{BO} counterparts. This is due to two difficulties. First, imidazole is an oblate molecule, and there are large rotations of the PAS upon isotopic substitution, see Table S5 of the Supporting Information. In particular, when the C_5 carbon atom is substituted, the axes *a* and *b* are switched. Then, there are several small Cartesian coordinates, especially $b(N_3) = 0.202$ Å, $a(C_2) = 0.220$ Å, and $a(H_2) = 0.348$ Å. This is enough to hamper an accurate determination of r_e^{SE} of this molecule.

At this stage, it is useful to determine an $r_m^{(2r)}$ structure. Usually it is hoped that the $r_m^{(2r)}$ structure determination would help to better analyze the origin of problems associated with the r_e^{SE} structure. As shown in Table 7, the $r_m^{(2r)}$ structure has exactly the same shortcomings as the r_e^{SE} structure; in particular, the C_4−C_5 bond length is much too short.

Nevertheless, it is possible to improve the semiexperimental fit. It is known that the computed rovibrational corrections are affected mainly by a systematic error, which is a few percent of the rovibrational correction.[43] As a consequence, the semiexperimental inertial defects are different from zero. It is worth correcting for this error by multiplying all the rovibrational corrections by a constant factor, $f = 0.960$ in this case; with this choice the equilibrium inertial defect of the parent species becomes zero. This correction reduces the standard deviations of the parameters but does not significantly affect their values. The next step forward is to use the mixed regression method.[29,71] In this method, some r_e^{BO} internal coordinates (called predicate observations, entered with an appropriate uncertainty) are fitted simultaneously with the semiexperimental moments of inertia. The uncertainties chosen for the rotational constant were (in kHz): 35 for *B* and 40 for *C*, and we increased the uncertainties of the *B* constants for isotopologues with a large PAS rotation. The uncertainty of the predicates was 0.002 Å for the bond lengths and 0.2° for the angles. This fit gives very satisfactory results and is given in the second-to-last column of Table 7. These parameters are considered to be the ones providing the best representation of the equilibrium structure of imidazole.

The lone pair of the N_1 nitrogen atom (pyrrolic nitrogen) in imidazole and pyrazole can contribute two electrons to the aromatic sextet. On the contrary, the second nitrogen atom (N_2 for pyrazole or N_3 for imidazole) has its lone pair localized in sp^2 orbitals. As a consequence, imidazole and pyrazole have structural properties intermediate between pyrrole and pyridine. For example, the C_2=N_3 bond length in imidazole at 1.311 Å and especially the N_2=C_3 bond length in pyrazole at 1.329 Å are close to the value found in pyridine, 1. 336 Å (see below, section 6.1). Furthermore, the N_1C_5 bond length in pyrazole at 1.352 Å or the N_1C_2 and N_1C_5 bond lengths in

dx.doi.org/10.1021/jp5084168 | J. Phys. Chem. A XXXX, XXX, XXX−XXX

Table 8. Structure of Pyridine[a]

	MP2(AE)		CCSD(T) AE	r_e^{BO} [b]	r_e^{SE}	$r_m^{(2)}$	r_s [c]
	CVTZ	wCVQZ	CVTZ				
N_1-C_2	1.3367	1.3338	1.3391	1.3362	1.3362(5)	1.3368(8)	1.3376(4)
C_2-C_3	1.3891	1.3865	1.3936	1.3910	1.3902(4)	1.3915(13)	1.3938(6)
C_3-C_4	1.3875	1.3848	1.3915	1.3889	1.3890(4)	1.3906(7)	1.3916(4)
C_2-H	1.0818	1.0807	1.0839	1.0828	1.0816(4)	1.0839(6)	1.0865(4)
C_3-H	1.0796	1.0785	1.0816	1.0805	1.0795(4)	1.0800(6)	1.0826(4)
C_4-H	1.0801	1.0790	1.0822	1.0811	1.0803(4)	1.0805(5)	1.0818(2)
$\angle C_3C_4H$	120.85	120.83	120.80	120.78	120.71(2)	120.78(3)	120.80(2)
$\angle C_3C_4C_5$	118.29	118.33	118.40	118.44	118.42(4)	118.44(6)	118.40(3)
$\angle C_4C_3H$	121.23	121.21	121.35	121.33	121.34(5)	121.27(6)	121.36(4)
$\angle C_2C_3C_4$	118.69	118.70	118.51	118.53	118.54(4)	118.51(6)	118.53(3)
$\angle C_2C_3H$	120.08	120.08	120.14	120.14	120.11(6)	120.22(7)	120.12(3)
$\angle C_3C_2H$	120.28	120.37	120.18	120.27	120.30(6)	120.31(7)	120.19(3)
$\angle NC_2C_3$	123.76	123.60	123.96	123.80	123.80(4)	123.78(6)	123.80(3)
$\angle NC_2H$	115.96	116.03	115.86	115.93	115.90(5)	115.91(6)	116.01(3)
$\angle C_2N_1C_6$	116.82	117.06	116.66	116.90	116.90(4)	116.97(6)	116.94(3)

[a]Distances in Å and angles in degrees. [b]From eq 1. [c]Reference 73.

imidazole at 1.360 and 1.375 Å, respectively, are close to the value found in pyrrole, 1.369 Å.

6. SIX-MEMBERED RINGS

6.1. Structure of Pyridine. Pyridine is a basic N-heterocyclic compound of formula C_5H_5N (Figure 1). It is an important solvent and reagent, and its ring occurs in many compounds of importance for life.

Pyridine is a planar oblate top (κ = +0.848) with an equilibrium structure of point-group symmetry C_{2v}. Its rotational spectrum has been analyzed many times, results published prior to 2005 are reviewed by Ye et al.[72] Particularly relevant for the present study is the work of Mata et al.,[73] who investigated the spectra of the deuterated species between 14 and 27 GHz and determined a precise r_s structure. As a result of the analysis of FTIR spectra, rotational constants of excited vibrational states are also available for pyridine.[74] Nevertheless, these constants are not used during the present structural analysis. There is also an early gas electron diffraction (GED) study for the structure of this molecule from Pyckhout et al.,[75] where information from infrared data and ab initio computations was also utilized. In an influential paper from 1984, Pongor, Pulay, and Boggs[76] determined accurate r_e^{BO} estimates and a scaled quantum mechanical (SQM) force field[77,78] for pyridine, aiding the assignment of the vibrational spectrum of the molecule. Later, several higher-level ab initio and DFT computations were reported on the structure and the vibrational spectrum of pyridine.[79] All these studies agree that the main characteristic of the structure of pyridine, as compared to benzene, is that the ∠CNC angle is significantly smaller than 120°, its value being slightly smaller than 117°.

A new estimate to r_e^{BO} of pyridine was computed in this study using eq 3. The r_e^{BO}(III) structural parameters obtained are given in Table 8.

The ground-state rotational constants of the parent species were taken from ref 70. The ground-state rotational spectra of the isotopic species were refitted using as predicates the quartic centrifugal distortion constants derived from the harmonic force field computed at the B3LYP/6-311+G(3df,2pd) level of theory. The experimental frequencies were taken from ref 71, except for the D_5 species, which are from ref 80, and for the 4-^{13}C and ^{15}N species, which are from ref 81.

The anharmonic force fields of ten isotopologues were computed at the B3LYP/6-311+G(3df,2pd) level. The derived α-constants were combined with the experimental ground-state rotational constants to yield estimates of semiexperimental equilibrium rotational constants, which were also corrected for the electronic contribution. The experimental values of the molecular g-tensor are taken from ref 82 for the parent species and from ref 83 for the ^{15}N species. The ground-state and semiexperimental equilibrium rotational constants as well as the inertial defects are given in Table S6 of the Supporting Information. The experimental ground-state inertial defect is Δ_0 = +0.039 uÅ^2 for the parent species; after the rovibrational correction it becomes −0.015 uÅ^2, and after the electronic correction it is Δ_e = 0.0031 uÅ^2, that is, close to zero. Similar results are obtained for the isotopic species; the range of the equilibrium inertial defects is only 0.0014 uÅ^2. This confirms that the rovibrational correction is likely to be accurate and that the electronic correction, although small, is not negligible.

The semiexperimental structure of pyridine is determined by an iteratively reweighted least-squares fit using the biweight weighting scheme. The structural parameters obtained are given in Table 8. The weight assigned to each datum in the final iteration is very similar and close to one, the only exceptions being the A rotational constants of the species D_2, D_3, and $^{13}C_3$, which have a slightly lower weight. Agreement between the r_e^{SE} and r_e^{BO} structures is almost perfect. Again, this is related to the good conditioning of the least-squares system. The r_s structure of Mata et al.[73] is also given in Table 8. It is worth emphasizing the surprisingly high consistency of the angle estimates. The empirical $r_m^{(2)}$ structure is also given in Table 8. It is interesting to note that it is in surprisingly good agreement with the equilibrium structure, with the exception of the CH bond lengths.

Comparison of the structure of pyridine with that of benzene, for which r_e(CC) = 1.392 Å and r_e(CH) = 1.081 Å,[84] shows that neither the CC nor the CH bond lengths are affected much by the single CH → N substitution. It is still interesting to note that the decreased π-electron density of pyridine as compared to benzene leads to a very slight contraction, instead of elongation, of r_e(CC), to 1.390 Å on average. The ring is strongly distorted at the ipso angle; ∠CNC is smaller than 120° by 3.1°, and the ortho inner-ring angle,

dx.doi.org/10.1021/jp5084168 | J. Phys. Chem. A XXXX, XXX, XXX−XXX

Table 9. Equilibrium Structural Parameters of Pyrimidine[a]

method	CCSD(T)	MP2	MP2	MP2	MP2	diff.[b]	CCSD(T)	r_e^{BO}(II)[c]	r_e^{SE} [d]
approx.[e]	FC	AE	FC	FC	FC		AE[f]		
basis set	VQZ	wCVQZ	wCVQZ	VQZ	AV5Z		wCVQZ		
$N_1-C_2 = N_3-C_2$	1.3369	1.3310	1.334	1.3343	1.3341	−0.0002	1.3338	1.3339	1.3331(3)
$N_1-C_6 = N_3-C_4$	1.3380	1.3322	1.3353	1.3356	1.3354	−0.0002	1.3349	1.3349	1.3349(6)
C_4-C_5	1.3907	1.3828	1.3861	1.3865	1.3863	−0.0002	1.3873	1.3874	1.3874(4)
C_2-H_2	1.0833	1.0800	1.0814	1.0815	1.0815	0.0000	1.0818	1.0819	1.0820(23)
$C_4-H_4 = C_6-H_6$	1.0839	1.0805	1.0820	1.082	1.0821	0.0001	1.0825	1.0824	1.0843(17)
C_5-H_5	1.0808	1.0776	1.0791	1.0792	1.0793	0.0001	1.0793	1.0793	1.0799(23)
$\angle N_1C_2N_3$	127.50	127.05	127.16	127.16	127.07	−0.087	127.393	127.393	127.364(38)
$\angle C_6N_1C_2$	115.58	115.93	115.86	115.86	115.93	0.068	115.655	115.656	115.712(21)
$\angle N_1C_6C_5$	122.36	122.06	122.09	122.09	122.00	−0.032	122.330	122.332	122.276(19)
$\angle C_4C_5C_6$	116.62	116.96	116.94	116.94	116.96	0.015	116.637	116.632	116.661(36)
$\angle N_1C_2H_2$	116.25	116.47	116.42	116.42	116.46	0.043	116.304	116.303	116.318(19)
$\angle C_5C_4H_4$	121.22	121.35	121.36	121.36	121.39	0.032	121.205	121.207	121.24(20)
$\angle C_4C_5H_5$	121.69	121.52	121.53	121.53	121.52	−0.007	121.682	121.684	121.670(18)

[a]Distances in Å and angles in degrees. [b]MP2(FC)/AV5Z − MP2(FC)/VQZ. [c]See eq 2. [d]See text and Table S7 of the Supporting Information. [e]AE = all electrons correlated; FC = frozen core approximation. [f]r_e^{BO}(I), see eq 1.

∠NCC, is larger than the reference 120° value by 3.8°. It is somewhat unusual that the substitution effect at the ortho position exceeds that at the ipso one.

6.2. Structure of Pyrimidine. Pyrimidine, *c*-$C_4H_4N_2$, is an aromatic N-heterocyclic compound with its two nitrogen atoms at meta position. The other two possible diazines are pyrazine and pyridazine, whose structures have been investigated before,[10,85] though not to the extent provided here. Because of a double CH → N substitution, the π-electron density in pyrimidine decreases further as compared to pyridine, resulting in much lower basicity.

The MW spectrum of pyrimidine was first analyzed by Blackman et al.[86] Later, Caminati and Damiani[87] measured the spectra of the ^{15}N and one ^{13}C isotopic species. More recently, Kisiel et al.[88] extended these measurements and obtained the rotational constants of all singly substituted ^{13}C- and ^{15}N-isotopic species in natural abundance. They determined a heavy-atom empirical r_0 structure. The structure of pyrimidine was also determined by combined analysis of data obtained by GED, rotational spectroscopy, and liquid-crystal NMR.[89] As a result of the analysis of FTIR spectra, rotational constants of excited vibrational states are also available for pyrimidine.[90] These constants are not used during the present structural analysis.

Estimates to r_e^{BO} of pyrimidine were computed using eqs 1 and 2. The corresponding r_e^{BO}(I) and r_e^{BO}(II) structural parameters are given in Table 9. The anharmonic force fields of the five isotopologues analyzed in ref 86 were computed at the B3LYP/6-311+G(3df,2pd) level. The derived α-constants were combined with the experimental ground-state rotational constants to yield estimates of semiexperimental equilibrium rotational constants, which were also corrected for the electronic contribution. As there are no experimental values for the molecular *g*-tensor, they were calculated at the B3LYP/6-311+G(3df,2pd) level of theory with Gaussian09. The results are g_{aa} = −0.100, g_{bb} = −0.122, and g_{cc} = 0.031. The ground-state and semiexperimental equilibrium rotational constants as well as the inertial defects are given in Table S7 of the Supporting Information. The experimental ground-state inertial defect is Δ_0 = +0.0350 uÅ^2 for the parent species; after the rovibrational correction it becomes −0.0141 uÅ^2, and after the electronic correction it is Δ_e = −0.0016 uÅ^2, that is, practically zero once again. This suggests that in the present case the electronic correction is not negligible. As the rotational constants of the deuterated species are not known, it is not possible to determine a complete semiexperimental structure. However, as for imidazole, the mixed regression method may be used. The predicate observations are the r_e^{BO} internal coordinates from Table 9 with an uncertainty of 0.002 Å for the bond lengths and 0.2° for the angles. The final uncertainty retained for the rotational constant was (in kHz): 50 for *A*, 20 for *B*, and 40 for *C*. Several trials were made starting with a minimum set of predicates, that is, the four internal coordinates locating the hydrogen atoms: C_2H_2, $C_4H_4 = C_6H_6$, C_5H_5, and $\angle N_3C_4H_4 = \angle N_1C_6H_6$. Then, the number of predicates was increased to the maximum number of nine. All the fits give compatible results, which are in good agreement with the r_e^{BO} structure. The results presented in the last column of Table 9 correspond to the fit with the complete set of predicates.

6.3. Structure of Uracil. Uracil, $C_4H_4N_2O_2$ (Figure 1), is a pyrimidine derivative that is one of the four nucleobases forming RNAs. While it is not a simple N-heterocyclic molecule like the others investigated in this study, we decided to include it in this study as it is a molecule whose structure and vibrational fundamentals have been investigated by Boggs et al.,[91] and knowledge of the accurate structure and spectra of uracil is indeed very important.

The MW spectrum of uracil was first recorded by Brown et al.[92] using a Stark spectrometer. More recently, the jet-cooled rotational spectrum has been measured using laser ablation molecular beam FTMW spectroscopy.[93] The spectra of the ^{13}C, ^{15}N, and ^{18}O isotopic species were also measured permitting the determination of an empirical r_s structure. A partial r_e^{SE} structure was calculated with the help of a cubic force field computed at the B3LYP/N07D level of theory.[94] In the same work, the structure was also computed at the CCSD(T) level, in conjunction with correlation-consistent basis sets (cc-pV*n*Z, with *n* = 3(T) and 4(Q)), taking also into account the core−valence correlation effects with the wCVTZ basis and the corrections due to diffuse functions using the AVTZ basis. Recently, the accuracy of the r_e^{BO} structure estimate was significantly improved using the larger wCVQZ basis set for the estimation of the core correlation and the AwCVQZ basis set

dx.doi.org/10.1021/jp5084168 | J. Phys. Chem. A XXXX, XXX, XXX−XXX

Table 10. Structure of Uracil[a]

method	r_e^{BO}			GED	r_e^{SE}	
	ref 94	ref 95	this work	ref 95	ref 94	this work
N_1-C_2	1.3785	1.3796	1.3807	1.381(2)	1.3818(5)	1.3810(6)
C_2-N_3	1.3756	1.3775	1.3774	1.379(2)		1.3749(7)
N_3-C_4	1.3974	1.4005	1.3993	1.402(2)	1.3979(4)	1.3991(6)
C_4-C_5	1.4539	1.4578	1.4558	1.454(8)	1.4550(6)	1.4548(6)
C_5-C_6	1.3433	1.3446	1.3435	1.339(18)	1.3450(6)	1.3429(7)
N_1-C_6	1.3723	1.3729	1.3726	1.374(2)	1.3720(6)	1.3722(7)
C_2-O_7	1.2112	1.2111	1.2099	1.210(1)	1.2103(2)	1.2101(4)
C_4-O_8	1.2138	1.2131	1.2126	1.212(1)	1.2128(2)	1.2186(4)
N_1-H	1.0046	1.0048	1.0045	1.005(10)	1.0043(12)	
N_3-H	1.0090	1.0090	1.0088	1.009(10)	1.0083(12)	
C_5-H	1.0766	1.0764	1.0761	1.076(13)	1.0757(12)	
C_6-H	1.0793	1.0794	1.0792	1.079(3)		1.0781(12)
$\angle C_2N_1C_6$	123.38	123.60	123.45	123.8(3)	123.37(2)	123.39(4)
$\angle N_1C_6C_5$	121.91	121.68	121.93	121.6(4)	121.92(1)	121.90(2)
$\angle C_4C_5C_6$	119.49	119.66	119.58	120.0(3)	119.52(2)	119.61(3)
$\angle C_5C_4N_3$	113.97	113.82	113.76	113.6(3)	113.86(2)	113.75(4)
$\angle C_4N_3C_2$	127.75	127.73	127.97	128.0(3)	127.942	127.97(4)
$\angle N_1C_2N_3$	113.51	113.51	113.32	113.0(2)	113.383	113.38(4)
$\angle N_3C_2O_7$	123.62	123.68	123.76	124.4(5)	123.88(4)	123.84(5)
$\angle C_5C_4O_8$	125.83	125.77	125.85	126.5(6)	125.77(5)	125.84(4)
$\angle C_2N_1H$	115.22	115.12	115.25	115.2(6)		115.14(12)
$\angle C_2N_3H$	115.7	115.70	115.60	114(7)		115.62(13)
$\angle C_6C_5H$	122.11	122.01	122.00	122		122.12(11)
$\angle N_1C_6H$	115.34	115.50		112(4)		115.39(6)
$\angle N_1C_2O_7$		122.81	122.92	122.6(5)		122.78(5)

[a]Distances in Å and angles in degrees.

for the effects of the diffuse functions.[95] The correction due to the diffuse functions was found in this study negligibly small.

To extend previous work and further improve the accuracy of the r_e structure estimate of uracil, we computed the effect of basis set enlargement VQZ → AV5Z at the MP2 level. The correction is quite small, always smaller than 0.001 Å for the bond lengths; the largest change is a decrease of the angle $\angle C_2N_3C_4$ by 0.12°. Finally, the r_e^{BO} structure is obtained using the equation

$$r_e^{BO} = \mathrm{CCSD(T)/CVTZ\_AE} + \mathrm{MP2(AE)} /[\mathrm{wCVQZ} - \mathrm{CVTZ}] + \mathrm{MP2(FC)} /[\mathrm{AV5Z} - \mathrm{VQZ}] \quad (7)$$

The results are given in Table 10, where they are compared with those of previous determinations.

The structure of uracil is defined by 21 independent internal coordinates. The rotational constants are available for 10 isotopologues; this only gives 20 independent rotational constants, because the molecule is planar at equilibrium. Furthermore, no rotational constants are available for the deuterated species. In their fits, Puzzarini and Barone[94] had to fix several parameters. In similar situations it is advantageous to use the mixed regression method, and this was done here. First, we redid the fits of the rotational transitions[93] using the method of predicate observations, with the quartic centrifugal distortion constants derived from a quadratic B3LYP/6-311+G(3df,2pd) force field. As there are no experimental values for the molecular g-tensor, they were also calculated at the B3LYP/6-311+G(3df,2pd) level of theory with Gaussian09. The results are $g_{aa} = -0.054$, $g_{bb} = -0.048$, and $g_{cc} = -0.013$. The uncertainties chosen for the rotational constants were (in kHz): 30 for A, 20 for B, and 10 for C. The uncertainties of the predicates were chosen to be 0.002 Å for the bond lengths and 0.2° for the angles. This set of data and uncertainties gives a good fit, whose results are also given in Table 10. The experimental ground-state and semiexperimental equilibrium rotational constants, as well as the inertial defects and the residuals of the fit, are given in Table S8 of the Supporting Information. This semiexperimental structure is in perfect agreement with our r_e^{BO} structure; it is also in good agreement with the GED structure, especially for the angles, but it is significantly more accurate.

It is tempting to compare the structure of uracil with that of pyrimidine, because they share the same ring skeleton. However, the two molecules have rather different structures because only pyrimidine is aromatic, with inner-ring bond lengths being intermediate between single and double bonds. For instance, the length of the N_1C_2 bond in pyrimidine is 1.334 Å, which is definitely shorter than a single bond, whereas in uracil it is 1.381 Å, which is a value typical of a single bond albeit shortened by the presence of the adjacent C═O bond. Likewise, the C_5C_6 bond length at 1.343 Å in uracil is close to a double bond value, whereas in pyrimidine it is much longer, its value being 1.387 Å.

7. SEVEN-MEMBERED RING: 1*H*-AZEPINE

There are four possible structural isomers (1*H*-, 2*H*-, 3*H*-, and 4*H*-azepine), but only 1*H*-azepine (called azepine hereafter) is investigated here. Planar 1*H*-azepine would be antiaromatic, and thus the molecule distorts into a boat form and assumes a geometry with a plane of symmetry perpendicular to the

dx.doi.org/10.1021/jp5084168 | J. Phys. Chem. A XXXX, XXX, XXX−XXX

Table 11. Equilibrium Structural Parameters of Azepine[a]

method	CCSD(T)_FC	MP2(FC)	MP2(FC)	MP2(FC)	MP2(AE)	r_e^{BO} [b]
basis set	VTZ	VTZ	AVQZ	wCVQZ	wCVQZ	
N_1-C_2	1.4216	1.4187	1.4154	1.4149	1.4113	1.4147
N_1-H	1.0077	1.0079	1.0070	1.0066	1.0053	1.0055
C_2-C_3	1.3441	1.3444	1.3428	1.3416	1.3383	1.3392
C_2-H	1.0854	1.0845	1.0841	1.0836	1.0821	1.0835
C_3-C_4	1.4673	1.4520	1.4500	1.4495	1.4466	1.4624
C_3-H	1.0835	1.0818	1.0817	1.0811	1.0796	1.0819
C_4-C_5	1.3501	1.3533	1.3515	1.3503	1.3467	1.3447
C_4-H	1.0852	1.0835	1.0832	1.0827	1.0812	1.0834
$\angle C_2N_1C_7$	116.16	113.36	114.01	113.83	114.12	117.10
$\angle C_2N_1H$	110.88	110.86	111.29	111.20	111.38	111.49
$\angle N_1C_2C_3$	124.27	122.80	122.94	122.90	123.01	124.53
$\angle N_1C_2H$	115.02	116.93	116.70	116.79	116.73	114.74
$\angle C_3C_2H$	120.02	120.27	120.35	120.31	120.26	120.05
$\angle C_2C_3C_4$	125.24	124.65	124.79	124.75	124.78	125.41
$\angle C_2C_3H$	117.03	117.08	116.93	116.98	116.97	116.87
$\angle C_4C_3H$	117.72	118.27	118.27	118.27	118.25	117.71
$\angle C_3C_4C_5$	125.17	124.80	124.85	124.83	124.85	125.25
$\angle C_3C_4H$	116.50	117.05	117.02	117.02	117.00	116.45
$\angle C_5C_4H$	118.27	117.98	117.97	117.98	117.99	118.26
$C_7N_1C_2C_3$	55.94	62.29	61.25	61.54	60.97	54.33
$C_7N_1C_2H$	−125.31	−118.78	−120.01	−119.53	−120.02	−127.02
HN1C2C3	−176.30	−172.28	−171.88	−171.93	−171.85	−175.83
HN_1C_2H	2.45	6.65	6.86	6.99	7.16	2.82
$N_1C_2C_3C_4$	−0.26	−2.12	−1.67	−1.76	−1.48	0.47
$N_1C_2C_3H$	178.27	177.32	177.43	177.45	177.60	178.53
$HC_2C_3C_4$	178.95	178.99	179.63	179.34	179.54	179.78
HC_2C_3H	−0.43	−1.57	−1.27	−1.44	−1.37	−0.06
$C_2C_3C_4C_5$	−32.08	−33.64	−33.46	−33.55	−33.54	−31.89
$C_2C_3C_4H$	150.67	151.24	151.42	151.30	151.18	150.73
$HC_3C_4C_5$	149.40	146.93	147.45	147.25	147.39	150.06
HC_3C_4H	−27.84	−28.19	−27.68	−27.91	−27.89	−27.31
$C_3C_4C_5C_6$	0.00	0.00	0.00	0.00	0.00	0.00
$HC_4C_5C_6$	177.20	175.07	175.08	175.11	175.24	177.33
HC_4C_5H	0.00	0.00	0.00	0.00	0.00	0.00

[a]Distances in Å and angles in degrees. [b]CCSD(T)_FC/VTZ + MP2(FC)/[AVQZ − VTZ] + MP2(AE)/wCVQZ − MP2(FC)/wCVQZ.

assumed plane of the carbon atoms. Note that stable derivatives of azepine have been shown to be nonplanar.

We are not aware of any experimental structural results for azepine, a ring with C_s point-group symmetry, where the symmetry plane is "perpendicular" to the assumed plane of the heavy atoms of the ring.

Geometry optimizations have been reported for azepine at the MCSCF/6-31G(d,p), the B3LYP/6-311++G**, and the MP2/6-311++G** levels of electronic structure theory.[96,97] As azepine is significantly larger than the other molecules of this work, its r_e^{BO} structure was first estimated in the FC approximation using the VTZ basis set and the CCSD(T) method. The core−core and core−valence correlation corrections were computed at the MP2 level using the wCVQZ basis set, and the small effect of further basis set enlargement was also computed at the MP2 level using the AVQZ basis set. The final r_e^{BO} structure estimate is given by the equation

$$r_e^{BO} = \text{CCSD(T)\_FC/VQZ} + \text{MP2(AE)/wCVQZ} - \text{MP2(FC)/wCVQZ} + \text{MP2(FC)/AVQZ} - \text{MP2(FC)/VTZ} \quad (8)$$

The most important structural parameters obtained are given in Table 11. The first obvious conclusion is that azepine is definitely nonplanar; most of the torsional angles deviate significantly from 0 or 180°. Furthermore, the C−C single bonds $r(C_3-C_4) \equiv r(C_5-C_6)$ at 1.467 Å are much longer than the C=C double bonds $r(C_2=C_3) \equiv r(C_6=C_7)$ at 1.344 Å and $r(C_4=C_5)$ at 1.350 Å. The value found for the r(C−N) bond length at 1.415 Å is typical for a single bond. It is also worth noting that the MP2 method does not seem to be able to predict the torsional angles with the usual accuracy; the deviations may approach 7°.

8. CONCLUSIONS

In this study highly accurate equilibrium structures have been derived for the following N-heterocycles: 1*H*- and 2*H*-azirine, aziridine, azete, pyrrole, pyrazole, imidazole, pyridine, pyrimidine, uracil, and 1*H*-azepine. For several of these molecules not only r_e^{BO} but also r_e^{SE} estimates of equilibrium structures could be determined. All equilibrium structures agree nicely with each other confirming the accuracy of their determination.

The present investigation resulted in, as well as confirmed, a number of methodological findings significant for structural determinations of semirigid molecules. These can be

dx.doi.org/10.1021/jp5084168 | J. Phys. Chem. A XXXX, XXX, XXX−XXX

summarized as follows: (1) The all-electron CCSD(T) method with the wCVQZ basis set yields highly satisfactory structural results for all the molecules investigated. It is found that the extension to larger basis sets does not significantly improve the accuracy of the results, because the small correction when going from VQZ to V5Z basis is almost completely compensated by the effect of diffuse functions when going from V5Z to AV5Z basis. The CCSD(T) method with the VQZ basis set in the frozen-core approximation and a core correction calculated at the MP2/wCVQZ level gives results of comparable quality. Of importance for later structural studies of even larger systems is the fact that it is also possible to use the CCSD(T) method with the smaller wCVTZ basis set, all electrons correlated, and the effect of further basis set enlargement, wCVTZ → wCVQZ, calculated at the MP2 level. This cheaper method is almost as accurate as the previous ones. (2) The semiexperimental method gives results of at least the same accuracy provided a full data set of accurate ground-state rotational constants is available. This study confirms that it is highly desirable to have accurate ground-state rotational constants to determine an accurate structure, although this may often imply refitting the spectroscopic constants to measured spectra to obtain more reliable rotational constants. (3) It must be noted that, at least for this class of compounds, the empirical mass-dependent method (r_m) also delivers rather accurate estimates of equilibrium structures. This useful observation may be connected to the fact that the least-squares systems used for the structural refinements are well-conditioned.

The present study also offers several chemical insights. Although it has been utilized for a long time, the geometry of the molecule may not be a good indicator of its aromaticity.[98,99] However, it is interesting to have a look at the bond lengths of adjacent bonds because aromaticity often implies a tendency to bond length equalization. The antiaromatic molecules 2*H*-azirine and azete have extremely different CN bond lengths; in particular, both molecules have a very long single bond. The nonaromatic molecule aziridine has a CN bond length of 1.470 Å, close to the value found in methylamine, 1.462 Å. The aromatic compounds show very small differences between the lengths of the adjacent bonds, which are intermediate between single and double bonds. Finally, the case of uracil is interesting because, contrary to pyrimidine, it is not aromatic. Nevertheless, the N_1C_2 and N_1C_6 bond lengths differ by only 0.008 Å.

■ ASSOCIATED CONTENT

Supporting Information

Eight tables, separated by molecules. They include ground state and semiexperimental rotational constants, rovibrational corrections, residuals of the structural fits, equilibrium inertial defects Δ_e, and angles of rotation of the principal axis system upon isotopic substitution for the molecules of this study. This material is available free of charge via the Internet at http://pubs.acs.org.

■ AUTHOR INFORMATION

Corresponding Author

*E-mail: csaszar@chem.elte.hu.

Notes

The authors declare no competing financial interest.

■ ACKNOWLEDGMENTS

Part of the research described has been supported by the Scientific Research Fund of Hungary (Grant No. OTKA NK83583).

■ REFERENCES

(1) Pyykkö, P.; Riedel, S.; Patzschke, M. Triple-Bond Covalent Radii. *Chem.—Eur. J.* **2005**, *11*, 3511−3520.
(2) Carter, S.; Mills, I.; Handy, N. C. The Equilibrium Structure of HCN. *J. Chem. Phys.* **1992**, *97*, 1606−1607.
(3) Botschwina, P.; Horn, M.; Seeger, S.; Flügge, J. Equilibrium Geometry of HC_3N. *Mol. Phys.* **1993**, *78*, 191−198.
(4) Rudolph, H. D.; Demaison, J.; Császár, A. G. Accurate Determination of the Deformation of the Benzene Ring upon Substitution: Equilibrium Structures of Benzonitrile and Phenylacetylene. *J. Phys. Chem. A* **2013**, *117*, 12969−12982.
(5) Liévin, J.; Demaison, J.; Herman, M.; Fayt, A.; Puzzarini, C. Comparison of the Experimental, Semiexperimental and ab initio Equilibrium Structures of Acetylene: Influence of Relativistic Effects and of the Diagonal Born-Oppenheimer Corrections. *J. Chem. Phys.* **2011**, *134*, 064119.
(6) Demaison, J.; Császár, A. G.; Kleiner, I.; Møllendal, H. Equilibrium vs Ground State Planarity of the CONH Linkage. *J. Phys. Chem. A* **2007**, *111*, 2574−2586.
(7) Pyykkö, P.; Atsumi, M. Molecular Single-Bond Covalent Radii for Elements 1−118. *Chem.—Eur. J.* **2009**, *15*, 186−197.
(8) Krygowski, T. M.; Szatylowicz, H.; Stasyuk, O. A.; Dominikowska, J.; Palusiak, M. Aromaticity from the Viewpoint of Molecular Geometry: Application to Planar Systems. *Chem. Rev.* **2014**, *114*, 6383−6422.
(9) Chen, Z.; Wannere, C. S.; Corminboeuf, C.; Puchta, R.; Schleyer, P. v. R. Nucleus-Independent Chemical Shifts (NICS) as an Aromaticity Criterion. *Chem. Rev.* **2005**, *105*, 3842−3888.
(10) Esselman, B. J.; Amberger, B. K.; Shutter, J. D.; Daane, M. A.; Stanton, J. F.; Woods, R. C.; McMahon, R. J. Rotational Spectroscopy of Pyridazine and its Isotopologues from 235−360 GHz: Equilibrium Structure and Vibrational Satellites. *J. Chem. Phys.* **2013**, *139*, 224304.
(11) Demaison, J.; Császár, A. G.; Margulès, L. D.; Rudolph, H. D. Equilibrium Structure of Heterocyclic Molecules with Large Principal Axis Rotations upon Isotopic Substitution. *J. Phys. Chem. A* **2011**, *115*, 14078−14091.
(12) Demaison, J.; Jahn, M. K.; Cocinero, E. J.; Lesarri, A.; Grabow, H.-U.; Guillemin, J.-C.; Rudolph, H. D. Accurate Semiexperimental Structure of 1,3,4-Oxadiazole by the Mixed Estimation Method. *J. Phys. Chem. A* **2013**, *117*, 2278−2284.
(13) Legon, A. C. Equilibrium Conformations of Four- and Five-Membered Cyclic Molecules in the Gas Phase: Determination and Classification. *Chem. Rev.* **1980**, *80*, 231−262.
(14) *Equilibrium Molecular Structures;* Demaison, J.; Boggs, J. E.; Császár, A. G., Eds.; CRC Press: Boca Raton, FL, 2011.
(15) Purvis, G. D., III; Bartlett, R. J. A Full Coupled-Cluster Singles and Doubles Model: The Inclusion of Disconnected Triples. *J. Chem. Phys.* **1982**, *76*, 1910−1918.
(16) Raghavachari, K.; Trucks, G. W.; Pople, J. A.; Head-Gordon, M. A Fifth-Order Perturbation Comparison of Electron Correlation Theories. *Chem. Phys. Lett.* **1989**, *157*, 479−483.
(17) Császár, A. G.; Allen, W. D.; Schaefer, H. F., III In Pursuit of the ab initio Limit for Conformational Energy Prototypes. *J. Chem. Phys.* **1998**, *108*, 9751−9764.
(18) Allen, W. D.; East, A. L. L.; Császár, A. G. In *Structures and Conformations of Non-Rigid Molecules;* Laane, J., Dakkouri, M., van der Veken, B., Oberhammer, H., Eds.; Kluwer: Dordrecht, 1993; pp 343−373.
(19) Møller, C.; Plesset, M. S. Note on an Approximation Treatment for Many-Electron Systems. *Phys. Rev.* **1934**, *46*, 618−622.
(20) Dunning, T. H., Jr. Gaussian Basis Sets for Use in Correlated Molecular Calculations. I. The Atoms Boron through Neon and Hydrogen. *J. Chem. Phys.* **1989**, *90*, 1007−1023.

(21) Kendall, R. A.; Dunning, T. H., Jr.; Harrison, R. J. Electron Affinities of the First-Row Atoms Revisited. Systematic Basis Sets and Wave Functions. *J. Chem. Phys.* **1992**, *96*, 6796−6806.
(22) Woon, D. E.; Dunning, T. H., Jr. Gaussian Basis Sets for Use in Correlated Molecular Calculations. V. Core-Valence Basis Sets for Boron through Neon. *J. Chem. Phys.* **1995**, *103*, 4572−4585.
(23) Peterson, K. A.; T. H. Dunning, T. H., Jr. Accurate Correlation Consistent Basis Sets for Molecular Core−Valence Correlation Effects: The Second Row Atoms Al−Ar, and the First Row Atoms B−Ne Revisited. *J. Chem. Phys.* **2002**, *117*, 10548−10560.
(24) Császár, A. G.; Allen, W. D. The Effect of 1s Correlation on D_e, r_e, and ω_e of First-Row Diatomics. *J. Chem. Phys.* **1996**, *104*, 2746−2748.
(25) Stanton, J. F.; Gauss, J.; Harding, M. E.; Szalay, P. G. with contributions from Auer, A. A.; Bartlett, R. J.; Benedikt, U.; Berger, C.; Bernholdt, D. E.; Bomble, Y. J. et al. CFOUR, a Quantum Chemical Program Package for Performing High-Level Quantum Chemical Calculations on Atoms and Molecules. For the current version, see http://www.cfour.de (accessed June 19, 2013).
(26) Frisch, M. J.; Trucks, G. W.; Schlegel, H. B.; Scuseria, G. E.; Robb, M. A.; Cheeseman, J. R.; Scalmani, G.; Barone, V.; Mennucci, B.; Petersson., G. A. et al. *Gaussian09,* Rev. C.01; Gaussian, Inc.: Wallingford, CT, 2010.
(27) Pulay, P.; Meyer, W.; Boggs, J. E. Cubic Force Constants and Equilibrium Geometry of Methane from Hartree−Fock and Correlated Wavefunctions. *J. Chem. Phys.* **1978**, *68*, 5077−5085.
(28) Jaeger, H. M.; Schaefer, H. F., III; Demaison, J.; Császár, A. G.; Allen, W. D. Lowest-Lying Conformers of Alanine: Pushing Theory to Ascertain Precise Energetics and Semiexperimental r_e Structures. *J. Chem. Theory Comput.* **2010**, *6*, 3066−3078.
(29) Demaison, J. The Method of Least Squares. In *Equilibrium Molecular Structures;* Demaison, J., Boggs, J. E., Császár, A. G., Eds.; CRC Press: Boca Raton, FL, 2011; pp 29−52.
(30) Bartell, L. S.; Romanesko, D. J.; Wong, T. C. Augmented Analyses: Method of Predicate Observations. In *Chemical Society Specialist Periodical Report No. 20: Molecular Structure by Diffraction Methods;* Sims, G. A., Sutton, L. E., Eds.; The Chemical Society: London, 1975, Vol. 3, pp 72−79.
(31) Császár, A. G. Anharmonic Molecular Force Fields. *WIREs Comput. Mol. Sci.* **2012**, *2*, 273−289.
(32) Kohn, W.; Sham, L. J. Self-Consistent Equations Including Exchange and Correlation Effects. *Phys. Rev. A* **1965**, *140*, 1133−1138.
(33) Becke, A. D. Density-Functional Thermochemistry. III. The Role of Exact Exchange. *J. Chem. Phys.* **1993**, *98*, 5648−5652.
(34) Lee, C. T.; Yang, W. T.; Parr, R. G. Development of the Colle-Salvetti Correlation-Energy Formula into a Functional of the Electron Density. *Phys. Rev. B* **1988**, *37*, 785−789.
(35) Dressler, S.; Thiel, W. Anharmonic Force Fields from Density Functional Theory. *Chem. Phys. Lett.* **1997**, *273*, 71−78.
(36) Boese, A. D.; Klopper, W.; Martin, J. M. L. Assessment of Various Density Functionals and Basis Sets for the Calculation of Molecular Anharmonic Force Fields. *Int. J. Quantum Chem.* **2005**, *104*, 830−845.
(37) Allen, W. D.; Császár, A. G. On the ab initio Determination of Higher-Order Force Constants at Nonstationary Reference Geometries. *J. Chem. Phys.* **1993**, *98*, 2983−3015.
(38) Mills, I. M. Vibration-Rotation Structure in Asymmetric- and Symmetric-Top Molecules. In *Molecular Spectroscopy: Modern Research;* Rao, K. N., Mathews, C. W.; Eds.; Academic Press: New York, 1972; pp 115−140.
(39) Gordy, W.; Cook, R. L. *Microwave Molecular Spectra;* Wiley: New York, 1984; Chapter 11.
(40) Hamilton, L. C. *Regression with Graphics;* Duxbury Press: Belmont, CA, 1992.
(41) Kummli, D. S.; Frey, H. M.; Leutwyler, S. Femtosecond Degenerate Four-Wave Mixing of Carbon Disulfide: High-Accuracy Rotational Constants. *J. Chem. Phys.* **2006**, *124*, 144307.
(42) Kummli, D. S.; Frey, H. M.; Leutwyler, S. Accurate Determination of the Structure of 1,3,5-Trifluorobenzene by Femtosecond Rotational Raman Coherence Spectroscopy and ab initio Calculations. *Chem. Phys.* **2010**, *367*, 36−43 see Figures 5 and 6.
(43) Vogt, N.; Vogt, J.; Demaison, J. Accuracy of the Rotational Constants. *J. Mol. Struct.* **2011**, *988*, 119−127.
(44) Watson, J. K. G.; Roytburg, A.; Ulrich, W. Least-Squares Mass-Dependence Molecular Structures. *J. Mol. Spectrosc.* **1999**, *196*, 102−129.
(45) Lathan, W. A.; Radom, L.; Hariharan, P. C.; Hehre, W. J.; Pople, J. A. Structures and Stabilities of Three-Membered Rings from ab initio Molecular Orbital Theory. *Top. Curr. Chem.* **1973**, *40*, 1−45.
(46) Ford, R. G. Preparation, Dipole Moment, and Quadrupole Coupling Constant of 2*H*-Azirine. *J. Am. Chem. Soc.* **1977**, *99*, 2389−2390.
(47) Bogey, M.; Destombes, J.-L.; Denis, J.-M.; Guillemin, J.-C. The Millimeterwave Rotational Spectrum of 2*H*-Azirine. *J. Mol. Spectrosc.* **1986**, *115*, 1−14.
(48) Thorwirth, S.; Müller, H. S. P.; Winnewisser, G. The Millimeter- and Submillimeter-Wave Spectrum and the Dipole Moment of Ethylenimine. *J. Mol. Spectrosc.* **2000**, *199*, 116−123.
(49) Thorwirth, S.; Gendriesch, R.; Müller, H. S. P.; Lewen, F.; Winnewisser, G. Pure Rotational Spectrum of Ethylenimine at 1.85 THz. *J. Mol. Spectrosc.* **2000**, *201*, 323−325.
(50) Motyenko, R. A.; Margulès, L.; Alekseev, E. A.; Guillemin, J.-C.; Demaison, J. Centrifugal Distortion Analysis of the Rotational Spectrum of Aziridine: Comparison of Different Hamiltonians. *J. Mol. Spectrosc.* **2010**, *264*, 94−99.
(51) Ngom, M.; Kwabia-Tchana, F.; Perrin, A.; Guillemin, J.-C.; Flaud, J.-M.; Demaison, J.; Ngom, El. A. New Vibrational Assignments for the ν_1 to ν_{17} Vibrational Modes of Aziridine and First Analysis of the High-Resolution Infrared Spectrum of Aziridine between 720 and 1050 cm^{-1}. *Mol. Phys.* **2011**, *109*, 2153−2161.
(52) Bak, B.; Skaarup, S. The Substitution Structure of Ethylenimine. *J. Mol. Struct.* **1971**, *10*, 385−391.
(53) Sutter, D. H.; Flygare, W. H. Molecular *g* Values, Magnetic Susceptibility Anisotropies, Second Moment of the Charge Distribution, and Molecular Quadrupole Moments in Ethylenimine and Pyrrole. *J. Am. Chem. Soc.* **1969**, *91*, 6895−6902.
(54) Kummli, D. D.; Frey, H. M.; Keller, M.; Leutwyler, S. Femtosecond Degenerate Four-Wave Mixing of Cyclopropane. *J. Chem. Phys.* **2005**, *123*, 054308.
(55) Nygaard, L.; Nielsen, J. T.; Kirchheiner, J.; Maltesen, G.; Rastrup-Andersen, J.; Sørensen, G. O. Microwave Spectra of Isotopic Pyrroles. Molecular Structure, Dipole Moment, and ^{14}N Quadrupole Coupling Constants of Pyrrole. *J. Mol. Spectrosc.* **1969**, *3*, 491−506.
(56) Wlodarczak, G.; Martinache, L.; Demaison, J.; Van Eijck, B. P. The Millimeter-wave Spectra of Furan, Pyrrole, and Pyridine: Experimental and Theoretical Determination of the Quartic Centrifugal Distortion Constants. *J. Mol. Spectrosc.* **1988**, *127*, 200−208.
(57) Mellouki, A.; vander Auwera, J.; Herman, M. Rotation-Vibration Constants for the ν_1, ν_{22}, ν_{24}, $\nu_{22} + \nu_{24}$ and Ground States in Pyrrole. *J. Mol. Spectrosc.* **1999**, *193*, 195−203.
(58) Hegelund, F.; Larsen, R. W.; Palmer, M. H. The High-Resolution Infrared Spectrum of Pyrrole between 900 and 1500 cm^{-1} Revisited. *J. Mol. Spectrosc.* **2008**, *252*, 93−97.
(59) Palmer, M.; Larsen, R. W.; Hegelund, F. Comparison of Theoretical and Experimental Studies of Infrared and Microwave Spectral Data for 5- and 6-Membered Ring Heterocycles: The Rotation Constants, Centrifugal Distortion and Vibration Rotation Constants. *J. Mol. Spectrosc.* **2008**, *252*, 60−71.
(60) Väänänen, T.; Jokisaari, J.; Kääriänen, A.; Lounila, J. The Structure of Pyrrole-^{15}N Determined in Nematic Liquid Crystals Utilizing ^{13}C-satellites in ^{1}H NMR Spectra. *J. Mol. Struct.* **1983**, *102*, 175−182.
(61) Christiansen, O.; Gauss, J.; Stanton, J. F.; Jørgensen, P. The Electronic Spectrum of Pyrrole. *J. Chem. Phys.* **1999**, *111*, 525−537.
(62) Botschwina, P.; Oswald, R. Fulvenallenyl Cation ($C_7H_5^+$) and Its Complex with an Argon Atom: Results of High-Level Quantum-Chemical Calculations. *J. Phys. Chem. A* **2012**, *116*, 3448−3453.

(63) Kirchhoff, W. H. The Microwave Spectrum and Dipole Moment of Pyrazole. *J. Am. Chem. Soc.* **1967**, *89*, 1312−1316.
(64) Nygaard, L.; Christen, D.; Nielsen, J. T.; Pedersen, E. J.; Snerling, O.; Vestergaard, E.; Sørensen, G. O. Microwave Spectra of isotopic Pyrazoles and Molecular Structure of Pyrazole. *J. Mol. Struct.* **1974**, *22*, 401−413.
(65) Stolze, M.; Sutter, D. H. The Rotational Zeeman Effect of Pyrazole and Imidazole. *Z. Naturforsch., A* **1987**, *42*, 49−56.
(66) Böttcher, O.; Sutter, D. H. The ^{14}N Nuclear Quadrupole Coupling Tensors, the Tensors of the Molecular Magnetic Susceptibility and the Molecular Electric Quadrupole Moment in Pyrazole: A High Resolution Rotational Zeeman Effect Study. *Z. Naturforsch., A* **1990**, *45*, 1248−1258.
(67) Wlodarczak, G.; Demaison, J.; Van Eijck, B.; Zhao, M.; Boggs, J. E. Ab Initio and Experimental Quartic Centrifugal Distortion Constants of Acetone, Pyrazole and γ-Pyrone. *J. Chem. Phys.* **1991**, *94*, 6698−6707.
(68) Llamas-Saiz, A. L.; Foces-Foces, C.; Mó, O.; Yáñez, M.; Elguero, E.; Elguero, J. The Geometry of Pyrazole: a Test for ab initio Calculations. *J. Comput. Chem.* **1995**, *16*, 263−272.
(69) Blackman, G. L.; Brown, R. D.; Burden, F. R.; Elsum, I. R. Nuclear Quadrupole Coupling in the Microwave Spectrum of Imidazole. *J. Mol. Spectrosc.* **1976**, *60*, 63−70.
(70) Christen, D.; Griffiths, J. H.; Sheridan, J. The Microwave Spectrum of Imidazole; Complete Structure and the Electron Distribution from Nuclear Quadrupole Coupling Tensors and Dipole Moment Orientation. *Z. Naturforsch., A* **1981**, *37*, 1378−1385.
(71) Belsley, D. A. *Conditioning Diagnostics;* Wiley: New York, 1991.
(72) Ye, E.; Bettens, R. P. A.; De Lucia, F. C.; Petkie, D. T.; Albert, S. Millimeter and Submillimeter Wave Rotational Spectrum of Pyridine in the Ground and Excited Vibrational States. *J. Mol. Spectrosc.* **2005**, *232*, 61−65.
(73) Mata, F.; Quintana, M. J.; Sørensen, G. O. Microwave Spectra of Pyridine and Monodeuterated Pyridines. Revisited Molecular Structure of Pyridine. *J. Mol. Struct.* **1977**, *42*, 1−5.
(74) Albert, S.; Quack, M. High Resolution Rovibrational Spectroscopy of Chiral and Aromatic Molecules. *ChemPhysChem* **2007**, *8*, 1271−1281.
(75) Pyckhout, W. N.; Horemans, N.; Van Alsenoy, C.; Geise, H. J.; Rankin, D. W. H. The Molecular Structure of Pyridine in the Gas Phase Determined from Electron Diffraction, Microwave and Infrared Data and ab Initio Force Field Calculations. *J. Mol. Struct.* **1987**, *156*, 315−329.
(76) Pongor, G.; Pulay, P.; Boggs, J. E. Theoretical Prediction of Vibrational Spectra. I. The In-Plane Force Field and Vibrational Spectra of Pyridine. *J. Am. Chem. Soc.* **1984**, *106*, 2765−2769.
(77) Pulay, P.; Fogarasi, G.; Pongor, G.; Boggs, J. E.; Vargha, A. A Combination of Theoretical ab initio and Experimental Information to Obtain Reliable Harmonic Force Constants − Scaled Quantum Mechanical (SQM) Force Fields for Glyoxal, Acrolein, Butadiene, Formaldehyde, and Ethylene. *J. Am. Chem. Soc.* **1983**, *105*, 7037−7047.
(78) Allen, W. D.; Császár, A. G.; Horner, D. A. The Puckering Inversion Barrier and Vibrational Spectrum of Cyclopentene. A Scaled Quantum Mechanical Force Field Algorithm. *J. Am. Chem. Soc.* **1992**, *114*, 6834−6849.
(79) Szafran, M.; Koput, J. Ab Initio and DFT calculations of Structure and Vibrational Spectra of Pyridine and its Isotopomers. *J. Mol. Struct.* **2001**, *565*−*566*, 439−448.
(80) Spycher, R. M.; Petitprez, D.; Bettens, F. L.; Bauder, A. Rotational Spectra of Pyridine-(Argon)$_n$, n = 1, 2, Complexes and their Vibrationally Averaged Structures. *J. Phys. Chem. A* **1994**, *98*, 11863−11869.
(81) Bettens, R. P. A.; Bauder, A. The Microwave Spectrum and Structure of the Pyridine-CO Complex. *J. Chem. Phys.* **1995**, *102*, 1501−1509.
(82) Wang, J. H. S.; Flygare, W. H. Molecular *g* Values, Magnetic Susceptibility Anisotropies, Second Moments of the Electronic Charge Distribution, and Molecular Quadrupole Moments in Pyridine. *J. Chem. Phys.* **1970**, *52*, 5636−5640.
(83) Hamer, E.; Sutter, D. H. Molecular *g*-Values, Magnetic Susceptibility Anisotropies, Molecular Quadrupole Moments and Second Moments of the Electron Charge Distribution in Ethylene Oxide and Pyridine Isotopes. An Attempt to Determine the Sign of the Dipole Moment. *Z. Naturforsch., A* **1976**, *31*, 265−271.
(84) Demaison, J.; Rudolph, H. D.; Császár, A. G. Deformation of the Benzene Ring upon Fluorination: Equilibrium Structures of Fluorobenzenes. *Mol. Phys.* **2013**, *111*, 1539−1562.
(85) Bormans, B. J. M.; Dewith, G.; Mijlhoff, F. C. The Molecular Structure of Pyrazine as Determined from Gas-Phase Electron Diffraction Data. *J. Mol. Struct.* **1977**, *42*, 121−128.
(86) Blackman, G. L.; Brown, R. D.; Burden, F. R. The Microwave Spectrum, Dipole Moment, and Nuclear Quadrupole Coupling Constants of Pyrimidine. *J. Mol. Spectrosc.* **1970**, *35*, 444−454.
(87) Caminati, W.; Damiani, D. Easy Assignment of Rotational Spectra of Slightly Abundant Isotopic Species in Natural Abundance: ^{13}C and ^{15}N Isotopic Species of Pyrimidine. *Chem. Phys. Lett.* **1991**, *179*, 460−462.
(88) Kisiel, Z.; Pszczółkowski, L.; López, J. C.; Alonso, J. L.; Maris, A.; Caminati, W. Investigation of the Rotational Spectrum of Pyrimidine from 3 to 337 GHz: Molecular Structure, Nuclear Quadrupole Coupling, and Vibrational Satellites. *J. Mol. Spectrosc.* **1999**, *195*, 332−339.
(89) Cradock, S.; Liescheski, P. B.; Rankin, D. W. H.; Robertson, H. E. The r_α Structures of Pyrazine and Pyrimidine by the Combined Analysis of Electron Diffraction, Liquid-Crystal NMR, and Rotational Data. *J. Am. Chem. Soc.* **1988**, *110*, 2758−2763.
(90) Albert, S.; Quack, M. High Resolution Rovibrational Spectroscopy of Pyrimidine: Analysis of the B_1 modes ν_{10b} and ν_4 and B_2 mode ν_{6b}. *J. Mol. Spectrosc.* **2007**, *243*, 280−291.
(91) Harsányi, L.; Császár, P.; Császár, A.; Boggs, J. E. Interpretation of the Vibrational Spectra of Matrix-Isolated Uracil from Scaled ab initio Quantum Mechanical Force Fields. *Int. J. Quantum Chem.* **1986**, *29*, 799−815.
(92) Brown, R. D.; Godfrey, P. D.; McNaughton, D.; Pierlot, A. P. Microwave Spectrum of Uracil. *J. Am. Chem. Soc.* **1988**, *110*, 2329−2330.
(93) Vaquero, V.; Sanz, M. E.; López, J. C.; Alonso, J. L. The Structure of Uracil: A Laser Ablation Rotational Study. *J. Phys. Chem. A* **2007**, *111*, 3443−3445.
(94) Puzzarini, C.; Barone, V. Extending the Molecular Size in Accurate Quantum-Chemical Calculations: the Equilibrium Structure and Spectroscopic Properties of Uracil. *Phys. Chem. Chem. Phys.* **2011**, *13*, 7189−7197.
(95) Vogt, N.; Khaikin, L. S.; Grikina, O. E.; Rykov, A. N. A Benchmark Study of Molecular Structure by Experimental and Theoretical Methods: Equilibrium Structure of Uracil from Gas-Phase Electron Diffraction Data and Coupled-Cluster Calculations. *J. Mol. Struct.* **2013**, *1050*, 114−121.
(96) Toyota, A.; Koseki, S.; Umeda, H.; Suzuki, M.; Fujimoto, K. Pseudo-Jahn-Teller Distortion from Planarity in Heterocyclic Seven- and Eight-Membered Ring Systems with Eight π Electrons. *J. Phys. Chem. A* **2003**, *107*, 2749−2756.
(97) Dardonville, C.; Jimeno, M. L.; Alkorta, I.; Elguero, J. Homoheteroaromaticity: The Case Study of Azepine and Dibenzazepine. *Org. Biomol. Chem.* **2004**, *2*, 1587−1591.
(98) Chen, Z.; Wannere, C. S.; Corminboeuf, C.; Puchta, R.; Schleyer, P. v. R. Nucleus-Independent Chemical Shifts (NICS) as an Aromaticity Criterion. *Chem. Rev.* **2005**, *105*, 3842−3888.
(99) Kalescky, R.; Kraka, E.; Cremer, D. Description of Aromaticity with the Help of Vibrational Spectroscopy: Anthracene and Phenanthrene. *J. Phys. Chem. A* **2014**, *118*, 223−237.